

EMULSIFICATION MICROEXTRACTION USING
SURFACTANT COUPLED WITH COLORIMETRIC
DETECTION FOR DETERMINATION OF SYNTHETIC
DYES IN FOOD



Miss Niluh Indria Wardani

จุฬาลงกรณ์มหาวิทยาลัย
CHULALONGKORN UNIVERSITY

A Thesis Submitted in Partial Fulfillment of the Requirements
for the Degree of Master of Science in Chemistry
Department of Chemistry
FACULTY OF SCIENCE
Chulalongkorn University
Academic Year 2022
Copyright of Chulalongkorn University

การสกัดระดับจุลภาคด้วยการเกิดอิมัลชันโดยใช้สารลดแรงตึงผิวร่วมกับการตรวจวัดเชิงสีสำหรับการ
การตรวจวัดสี ย้อมสังเคราะห์ในอาหาร



วิทยานิพนธ์นี้เป็นส่วนหนึ่งของการศึกษาตามหลักสูตรปริญญาวิทยาศาสตรมหาบัณฑิต
สาขาวิชาเคมี ภาควิชาเคมี
คณะวิทยาศาสตร์ จุฬาลงกรณ์มหาวิทยาลัย
ปีการศึกษา 2565
ลิขสิทธิ์ของจุฬาลงกรณ์มหาวิทยาลัย

Thesis Title EMULSIFICATION MICROEXTRACTION USING
SURFACTANT COUPLED WITH COLORIMETRIC
DETECTION FOR DETERMINATION OF SYNTHETIC
DYES IN FOOD
By Miss Niluh Indria Wardani
Field of Study Chemistry
Thesis Advisor Associate Professor Dr. PAKORN VARANUSUPAKUL

Accepted by the FACULTY OF SCIENCE, Chulalongkorn University in Partial
Fulfillment of the Requirement for the Master of Science

..... Dean of the FACULTY OF SCIENCE
(Professor Dr. POLKIT SANGVANICH)

THESIS COMMITTEE

..... Chairman
(Professor Dr. ORAWON CHAILAPAKUL)
..... Thesis Advisor
(Associate Professor Dr. PAKORN VARANUSUPAKUL)
..... Examiner
(Associate Professor Dr. FUANGFA UNOB)
..... External Examiner
(Assistant Professor Dr. Wanida Wonsawat)



จุฬาลงกรณ์มหาวิทยาลัย
CHULALONGKORN UNIVERSITY

นิลู่ อินเดรีช วาร์ดานี : การสกัดระดับจุลภาคด้วยการเกิดอิมัลชันโดยใช้สารลดแรงดึงผิวร่วมกับการตรวจวัดเชิงสีสำหรับการตรวจวัดสี ซ้อมสังเคราะห์ในอาหาร. (EMULSIFICATION MICROEXTRACTION USING SURFACTANT COUPLED WITH COLORIMETRIC DETECTION FOR DETERMINATION OF SYNTHETIC DYES IN FOOD) อ.ที่ปรึกษาหลัก : รศ. ดร. ปกรณ์ วรรณสุภากุล

งานวิจัยนี้เป็นการพัฒนาเทคนิคการสกัดด้วยเฟสของเหลวระดับจุลภาคแบบอิมัลชันและการทำให้หยดตัวทำละลายอินทรีย์เป็นของแข็งลงร่วมกับการตรวจวัดภาพสีแบบดิจิทัลสำหรับการวิเคราะห์สีซ้อมสังเคราะห์ได้แก่ โรดามีน-บี และคริสตัลไวโอเล็ตในตัวอย่างอาหารและเครื่องสำอาง การสกัดใช้สารลดแรงดึงผิวชนิดกรดไขมันก่อให้เกิดอิมัลชันและทำการรวมหยดตัวทำละลายอิมัลชันและแยกออกจากชั้นตัวอย่างโดยทำให้เป็นของแข็งที่อุณหภูมิต่ำกว่าจุดเยือกแข็งของตัวทำละลาย หยดของแข็งจะถูกแยกและทำให้กลายเป็นของเหลวอีกครั้งก่อนนำไปหยดลงบนอุปกรณ์ตรวจวัดฐานกระดาษสำหรับการวิเคราะห์ภาพสีแบบดิจิทัล ศึกษาพารามิเตอร์ที่มีอิทธิพลต่อประสิทธิภาพในการสกัดโดยใช้วิธี response surface methodology-central composite design (RSM-CCD) ในการสกัดใช้ตัวอย่างปริมาตร 7 มิลลิลิตร ปรับสภาวะให้มีพีเอช 7 และ 8 ก่อนทำการสกัดคริสตัลไวโอเล็ตและโรดามีน-บี ตามลำดับ กรดออกทานอิกปริมาตร 21.6 ไมโครลิตรเป็นเฟสสกัด ทำให้เกิดอิมัลชันโดยการเขย่าอย่างแรงเป็นเวลา 10 วินาทีและปั่นเหวี่ยงที่ 3000 รอบต่อนาทีเป็นเวลา 5 นาที รูปภาพหยดสีถ่ายด้วยกล้องจากโทรศัพท์มือถือในกล่องที่มีการควบคุมแสง ระยะกล้องถึงรูปถ่ายที่ 36 เซนติเมตร วิเคราะห์ภาพหยดสีด้วยโปรแกรมอิมเมจ ซอส์แองด์ ซิดจำกัดในการตรวจวัดและซิดจำกัดในการหาปริมาณอยู่ที่ 0.8 ไมโครกรัมต่อลิตร และ 3 ไมโครกรัมต่อลิตรตามลำดับสำหรับการวิเคราะห์คริสตัลไวโอเล็ตและ 3 ไมโครกรัมต่อลิตร และ 10 ไมโครกรัมต่อลิตรตามลำดับสำหรับการวิเคราะห์โรดามีน-บี มีช่วงความเป็นเส้นตรงที่ 3 - 20 ไมโครกรัมต่อลิตร ($R^2 = 0.999$) สำหรับการวิเคราะห์คริสตัลไวโอเล็ต และ 10 - 40 ไมโครกรัมต่อลิตร ($R^2 = 0.995$) สำหรับการวิเคราะห์โรดามีน-บี. วิธีที่พัฒนานี้ได้นำไปใช้วิเคราะห์โรดามีน-บี ในตัวอย่างเครื่องสำอาง กลูม เซลล์ และซอสพริก และวิเคราะห์คริสตัลไวโอเล็ตในตัวอย่างน้ำดื่ม มีการได้กลับคืนสัมพัทธ์อยู่ระหว่าง 73-113 เปอร์เซ็นต์

จุฬาลงกรณ์มหาวิทยาลัย
CHULALONGKORN UNIVERSITY

สาขาวิชา เคมี
ปีการศึกษา 2565

ลายมือชื่อนิลิต
ลายมือชื่อ อ.ที่ปรึกษาหลัก

6372036523 : MAJOR CHEMISTRY

KEYWORD: microextraction; surfactant; emulsification; paper-based analytical device; food sample.

Niluh Indria Wardani : EMULSIFICATION MICROEXTRACTION USING SURFACTANT COUPLED WITH COLORIMETRIC DETECTION FOR DETERMINATION OF SYNTHETIC DYES IN FOOD. Advisor: Assoc. Prof. Dr. PAKORN VARANUSUPAKUL

In this thesis, solidification of floating organic drop-emulsification liquid-liquid microextraction (SFOD-ELLME) was combined with digital image colorimetry (DIC) for the analysis of synthetic dyes, such as rhodamine B (RhB) and crystal violet (CV) in food and drink samples. Here, the extraction was performed by using emulsified fatty acid surfactant and freezing procedure to separate the extracting phase. The solidified floating organic drop was then taken out, liquified and dropped on the paper platform for digital image colorimetric analysis. The response surface methodology-central composite design (RSM-CCD) was used to optimize some variables that influence the extraction efficiency. A sample of 7 mL was used and adjusted to pH 7 and 8 for CV and RhB, respectively prior to extraction. The extraction phase was 21.6 μL octanoic acid. The extraction phase was emulsified by manually shaking for 10 s and centrifugation at 3000 rpm for 5 min. The digital image was taken by the smartphone camera in the light-controlled box. The distance between camera and the paper platform was kept at 36 cm. The color was analyzed by ImageJ program using red channel. Limit of detection (LOD) and limit of quantification (LOQ) for CV were 0.8 $\mu\text{g/L}$ and 3 $\mu\text{g/L}$; 3 $\mu\text{g/L}$ and 10 $\mu\text{g/L}$ for RhB. The linear ranges were 3-20 $\mu\text{g/L}$ ($R^2 = 0.999$) for CV and 10-40 $\mu\text{g/L}$ ($R^2 = 0.995$) for RhB. The method was applied to determine RhB in beverage, candy, jelly, and chili sauce samples and CV in drinking water samples. The relative recovery percentages (RR%) between 73 % and 113 % were achieved.



Field of Study: Chemistry
Academic Year: 2022

Student's Signature
Advisor's Signature

ACKNOWLEDGEMENTS

The author would like to thank the department of chemistry at Chulalongkorn University and declares that I am a student under the scholarship program for ASEAN or Non – ASEAN Countries supported by Chulalongkorn University. Moreover, I want to express my gratitude to my advisor, Associate Professor Dr. Pakorn Varanusupakul who support and give me a lot of knowledge along my research journey until I can make this thesis. I also would like to give many thanks to my Thesis committee, Prof. Orawon Chailapakul, Associate Prof. Dr. Fuangfa Unob, and Assistant Prof. Dr. Wanida Wonsawat who give me insightful advice to improve my research and writing.

I really appreciate all my sisters and brothers in the laboratory from PV 1207 lab, PV 1205 lab, and CK 1218 lab. They give me mental support to never give up. I would like to give my special thanks to Dr. Waleed Alahmad and Dr. Ali Sahragard who give me insight and advice to finish my research, and also to Thidarat Sakumpim who help me a lot in the lab to communicate with Thai people and fill in documents with Thai language.

Furthermore, I send my gratitude and appreciation to my beloved parents and brother who as my support system since the beginning and forever. I am forever indebted to all those people who support me.

TABLE OF CONTENTS

	Page
.....	iii
ABSTRACT (THAI)	iii
.....	iv
ABSTRACT (ENGLISH)	iv
ACKNOWLEDGEMENTS	v
TABLE OF CONTENTS	vi
LIST OF TABLES	ix
LIST OF FIGURES	x
LIST OF ABBREVIATIONS	1
Chapter 1 Introduction	4
1.1 Introduction	4
1.2 Objectives	8
Chapter 2 Theory and literature review	9
2.1 Sample preparation	9
2.2 Surfactant	14
2.2.1 The roles of surfactant in sample preparation	18
2.2.2 Fatty acid as surfactant	18
2.3 Digital image colorimetry (DIC)	19
2.3.1 Definition and principal work	19
2.3.2 DIC method application	21
2.4 Synthetic dyes	22
2.4.1 Crystal Violet	26
2.4.2 Rhodamine B	27
2.5 RSM-CCD	28
Chapter 3 Methodology	29

3.1 Materials and chemicals	29
3.2 Apparatus and software	29
3.3 Fabrication of paper platform for droplet digital image colorimetry (DDIC) system	30
3.4 SFOD-ELLME-DDIC Procedure	30
3.5 Experimental design	32
3.6 Analytical performance	33
3.7 Sample analysis	34
3.7.1 Sample pre-treatment for samples of RhB	34
3.7.1.1 Beverage sample	34
3.7.1.2 Candy sample	34
3.7.1.3 Jelly sample	34
3.7.1.4 Chili sauce	34
3.7.2 Sample pre-treatment for samples of CV	34
3.7.2.1 Drinking water	34
3.8 Calculations	35
3.8.1 The relative recovery (RR%)	35
3.8.2 Enrichment factor (EF)	35
3.8.3 The extraction recovery (ER%)	36
3.8.4 Limit of Detection (LOD)	36
3.8.5 Limit of Quantification (LOQ)	36
Chapter 4 Results and discussions	37
4.1 Droplet digital image colorimetry	37
4.2 Optimization for solidification of floating organic drop-emulsification microextraction	38
4.2.1 Selection of color channel	38
4.2.2 Effect of extraction solvent type	40
4.2.3 Effect of manual shaking and centrifugation time	41
4.2.4 Effect of sample volume	43
4.2.5 Optimization of camera-paper platform distance	44

4.2.6 Experimental design.....	45
4.2.7 The effect of the region of interest (ROI) area in DIC analysis.....	48
4.3 Analytical features.....	50
4.4 Matrix effect analysis.....	51
4.5 Analysis of real samples.....	54
4.6 Significance and implications.....	55
Chapter 5 Conclusion.....	57
APPENDIX.....	58
REFERENCES.....	64
VITA.....	67



LIST OF TABLES

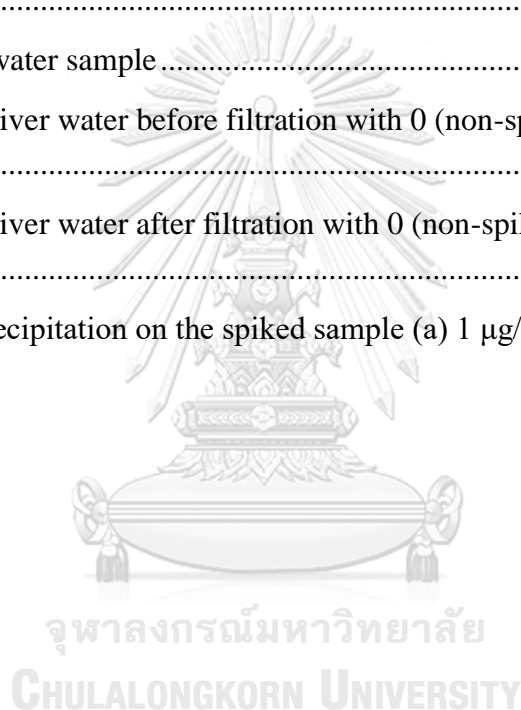
	Page
Table 1. The type of surfactants.....	17
Table 2. Classification of synthetic dyes based on the type of chromophore.....	23
Table 3. Analytical figures of merit of the developed SFOD-ELLME-DDIC procedure.....	51
Table 4. Determinations of RhB in several samples by SFOD-ELLME-DDIC (n=3).....	55
Table 5. Determinations of CV in drinking water sample by SFOD-ELLME-DDIC (n=3).....	55
Table 6. Several analytical methods for synthetic dyes analysis	56
Table 7. The experimental levels of the variable in the CCD.....	58
Table 8. The runs of CCD and the measured intensity of CV and RhB.....	58
Table 9. Analysis of Variance (ANOVA) of CCD.....	59
Table 10. One-way ANOVA result of ROI area.....	60
Table 11. List of dyes in the samples that is analyzed.....	61

LIST OF FIGURES

	Page
Figure 1. The classification of LPME.....	13
Figure 2. DLLME	14
Figure 3. The general structure of surfactant.....	16
Figure 4. Surfactant line up in the water-air interface	16
Figure 5. Procedure of smartphone digital image colorimetry	20
Figure 6. RGB color space cube	21
Figure 7. CV molecular structure.....	27
Figure 8. RhB molecular structure.....	27
Figure 9. CCD model (green dot are star point; red dots are high and low point; blue dot is central point)	28
Figure 10. The paper platform for the DDIC system.....	30
Figure 11. Schematic illustration of SFOD-ELLME-DDIC procedure.....	32
Figure 12. Schematic illustration of droplet digital image colorimetry (DDIC)	32
Figure 13. The comparison of final solution color intensity in (a) pre-wetted paper platform and (b) normal paper platform	38
Figure 14. (a) Puluz light box setup with the light source on the side of the box (b) droplet image when the light source is on the (i) top and (ii) side of the light box	38
Figure 15. The red, green, and blue intensity difference of the SFOD-ELLME-DDIC of (a) CV and (b) RhB; (condition: surfactant volume, 25 μ L; pH solution, 6; agitation time, 30 s; total volume, 5 mL; centrifugation rate, 3000 rpm; centrifugation time, 10 min; distance between the camera and paper platform, 25 cm).....	39
Figure 16. Effect of extraction solvent type in the SFOD-ELLME-DDIC of (a) CV and (b) RhB; (condition: surfactant volume, 25 μ L; concentration of CV and RhB, 40 μ g/L; pH solution, 6; agitation time, 30 s; total volume, 5 mL; centrifugation rate, 3000 rpm; centrifugation time, 10 min; distance between the camera and paper platform, 25 cm).....	40
Figure 17. Effect of shaking time in the SFOD-ELLME-DDIC of (a) CV and (b) RhB; (condition: extracting phase, octanoic acid; surfactant volume, 25 μ L; concentration of CV and RhB, 40 μ g/L; pH, 5; total volume, 5 mL; centrifugation	

rate, 3000 rpm; centrifugation time, 10 min; distance between the camera and paper platform, 25 cm).....	42
Figure 18. Effect of centrifugation time in the SFOD-ELLME-DDIC of (a) CV and (b) RhB; (condition: extracting phase, octanoic acid; surfactant volume, 25 μ L; concentration of CV and RhB, 40 μ g/L; pH, 5; shaking time, 10 s; total volume, 5 mL; centrifugation rate, 3000 rpm; distance between the camera and paper platform, 25 cm).	43
Figure 19. Effect of sample volume in the SFOD-ELLME-DDIC of (a) CV and (b) RhB; (condition: extracting phase, octanoic acid; centrifugation rate, 3000 rpm; surfactant volume, 25 μ L; concentration of CV and RhB, 40 μ g/L; pH solution, 6; shaking time, 10 s; centrifugation rate, 3000 rpm; centrifugation time, 5 min; distance between the camera and paper platform, 36 cm).	44
Figure 20. Optimization of camera-paper platform distance in the SFOD-ELLME-DDIC of (a) CV and (b) RhB; (condition: extracting phase, octanoic acid; surfactant volume, 25 μ L; concentration of CV and RhB, 40 μ g/L; pH, 5; shaking time, 10 s; total volume, 5 mL; centrifugation rate, 3000 rpm, centrifugation time, 5 min).	45
Figure 21. Pareto Chart of several affecting independent variable for (a) crystal violet and (b) rhodamine B	46
Figure 22. Response surface of sample pH and volume of extracting phase; (a) CV and (b) RhB.....	48
Figure 23. The effect of ROI area in the SFOD-ELLME-DDIC of (a) CV and (b) RhB; (condition: surfactant volume, 21.6 μ L; concentration of RhB, 40 μ g/L; concentration of CV, 20 μ g/L; pH, 8; shaking time, 10 s; total volume, 7 mL; centrifugation rate, 3000 rpm; centrifugation time, 5 min; distance between the camera and paper platform, 36 cm).	49
Figure 24. Calibration curve (a) CV 3-20 μ g/L and (b) RhB 10-40 μ g/L with (condition: sample volume, 7 mL; pH of sample, 7.0 for CV and 8.0 for RhB; extracting phase (octanoic acid) volume, 21.6 μ L; shaking time, 10 s; centrifugation time, 5 min; centrifugation rate, 3000 rpm; distance between the camera and paper platform, 36 cm).....	51
Figure 25. Matrix-matched calibration curve of real samples and external calibration curve of standard solution.	54
Figure 26. Crystal violet (a) microspecies distribution graph and (b) lipophilicity-pH graph (Chemicalize was used for calculating this property on 21 June 2022, https://chemicalize.com/ , developed by ChemAxon)	59
Figure 27. Dominant rhodamine B molecular structure in pH<3.5	60

Figure 28. Diagram of pH-lipophilicity of rhodamine B (Chemicalize was used for calculating this property on 21 June 2022, https://chemicalize.com/ , developed by ChemAxon).....	60
Figure 29. Figure of (a) molecular structure of capsanthin (b) the microspecies distribution of capsanthin in various pH (Chemicalize was used for calculating this property on 11 September 2022, https://chemicalize.com/ , developed by ChemAxon)	61
Figure 30. Residue from the extract from chili powder sample	61
Figure 31. figures of (a) aqueous extract from chili (b) microextraction result of aqueous extract.....	62
Figure 32. River water sample	62
Figure 33. Spike river water before filtration with 0 (non-spiked); 1 (10 $\mu\text{g/L}$); 2 (20 $\mu\text{g/L}$).....	62
Figure 34. Spike river water after filtration with 0 (non-spiked); 1 (10 $\mu\text{g/L}$); 2 (20 $\mu\text{g/L}$).....	62
Figure 35. The precipitation on the spiked sample (a) 1 $\mu\text{g/g}$ and (b) 2 $\mu\text{g/g}$	63



LIST OF ABBREVIATIONS

Abbreviation	Definition
μg	Microgram
ER%	Percentage of extraction recovery
RR%	Percentage of relative recovery
RSD%	Percentage of relative standard deviation
LD ₅₀	Lethal dose fifty
$^{\circ}\text{C}$	Degree of Celsius
ΔI	Color intensity (subtracted with blank)
ANOVA	Analysis of Variance
AOAC	Association of official analytical chemists
CCD	Central composite design
C-CD	Charge-coupled device
CE	Capillary electrophoresis
CIE	Commission Internationale de l'éclairage
CIS	Contact image sensor
CMOS	Complementary metal oxide semiconductor
CMYK	Cyan, magenta, yellow, and black
CV	Crystal violet
DAD	Diode array detector
DDIC	Droplet digital image colorimetry
DLLME	Dispersive liquid-liquid microextraction
DIC	Digital image colorimetry

EF	Enrichment factor
ELLME	Emulsification liquid-liquid microextraction
EFSA	European food safety authority
FDA	Food and drug administration
HF-LPME	Hollow fiber microextraction
HPLC	High-performance liquid chromatography
HSV	Hue, saturation, and value
HSB	Hue, saturation, and brightness
IARC	International agency for research on cancer
L	Liter
LED	Light emitting diodes
LLE	Liquid-liquid extraction
LOD	Limit of detection
LOQ	Limit of quantification
LPME	Liquid phase microextraction
L*a*b*	Lightness, color composition, and blue to yellow color intensity
MBE	Membrane-based extraction
min	Minute
OFAT	One factor at a time
PAD	Photodiode array detector
pH	Potenz of hydrogen/hydrogen concentration
pK _a	Negative logarithm value of acid dissociation constant

PTFE	Polytetrafluoroethylene
R	Red color channel intensity (not subtracted with blank)
R ²	Coefficient of determination
RhB	Rhodamine B
RGB	Red, green, blue
ROI	Region of interest
rpm	Rotation of minute
RSM	Response surface methodology
s	Second
SBSE	Stir bar solid-phase extraction
SD	Standard deviation
SDME	Single drop microextraction
SFE	Supercritical fluid extraction
SLE	Solid-liquid extraction
SPE	Solid phase extraction
SPME	Solid phase microextraction
SFOD-ELLME	Solidification of floating organic drop-emulsification liquid- liquid microextraction
UPLC	Ultra-performance liquid chromatography
TLC	Thin layer chromatography
UV-Vis	Ultraviolet-Visible spectroscopy
YUV	Brightness, blue-luminance components, red-luminance components

Chapter 1 Introduction

1.1 Introduction

Synthetic dyes have a wide range of applications in consumable products because they are less expensive compared to natural dyes¹. Considering that some synthetic dyes are carcinogenic and mutagenic to human and living things, and their uses in food and beverages are prohibited, quantification of their trace amount in such samples is critically needed for food safety and quality control^{2, 3}. Two examples of prohibited synthetic dyes that are illegally used in food products or foodstuffs and drinks are crystal violet (CV) and rhodamine B (RhB).

Analytical methods commonly used for determination of synthetic dyes are UV-Vis spectrophotometry⁴, high-performance liquid chromatography (HPLC)^{3, 5, 6}, ultra-performance liquid chromatography (UPLC)⁷, and capillary electrophoresis (CE)⁸ with UV/Vis detector. These methods are laborious, expensive, need a bulky instrument, and are not user-friendly. Therefore, the improvement in some aspects of analytical detection method is needed to provide sensitive and simple technique. Digital image colorimetry (DIC) could be considered as a simple alternative method for synthetic dyes detection¹.

Digital image colorimetry (DIC) is a quantitative method based on analysis of digital image reflecting light shown in red (R), green (G), and blue (B) intensity. DIC is a simple, rapid, and user-friendly detection method. The quantitative detection of dyes with DIC has been developed by coupling with a membrane filtration-enrichment technique⁹. Nevertheless, this method may fail to detect trace levels of

synthetic dyes from more complex food and drink samples. Food samples mostly have a complex matrix that may contain many components and interferences³

To develop the applicability of DIC for trace-level analysis of synthetic dyes, the proper sample preparation is needed depending on the sample matrix¹. Hence, suitable sample preparation should provide high enrichment factor and good selectivity for the proposed analytes (CV and RhB) prior to coupling with the DIC detection system.

Recently, ELLME has gained much attention due to its rapidity, high throughput, high sensitivity, environmentally friendliness, high enrichment factor, and simplicity. Consequently, the combination of ELLME and DIC would be interesting. In ELLME, the extraction phase is emulsified into very small droplets by chemicals or external forces. Conventional dispersive liquid-liquid microextraction (DLLME) is a common ELLME technique using disperser solvent to disperse the extracting solvent into the sample phase¹⁰. The main problem with DLLME using a disperser is the small partition coefficient of analyte to the organic solvent from the aqueous sample solution¹¹. Hence, the ELLME term was used in this research for focusing on the emulsification process and differentiating the proposed method from conventional DLLME.

The assisting of the emulsification using external force is preferred because it is more environmentally friendly with no need for a disperser solvent and other reagents³. External forces that can be used are ultrasound energy and vortex. Ultrasound tends to volatilize the organic acceptor phase and form a stable emulsion that is harder to separate and lengthens the separation time. Vortex-assisted liquid-liquid microextraction can enhance the solvent dispersion³ and improve extraction

efficiency. Besides, manual shaking could be an alternative way that is more convenient, rapid, and simple to facilitate emulsification.

The choice of appropriate acceptor phase or solvent would affect the performance of ELLME. The solvent should have low miscibility in water and high distribution ratio with analyte of interest, be able to disperse after adding chemical dispersants or external forces, compatible with the analytical instrument, and obtainable at a reasonable price¹². The acceptor phase can be classified into higher density and lower density than water. The lower-density solvent can be easily collected on top of the sample solution. The development of ELLME that uses low-density solvent is increasing nowadays¹⁰. Nevertheless, the separated phase collection of lower-density solvent is difficult. The solidification of floating organic drop (SFOD) has been proposed. In SFOD, the extracting phase was solidified at the temperature below its freezing point for collection or removal. Hence, the acceptor phase that is low-density solvent and high freezing point¹³ would be more preferable.

Surface-active agents (surfactants) are chemicals that have hydrophilic and hydrophobic moieties (amphiphile). Surfactants can be rendered into many forms in water such as liquid crystals, micelles, vesicles, and microemulsions. Surfactants could be used in sample preparation and give major benefits to minimizing the application of common organic solvents (e.g., chlorinated solvents). Surfactant can be used as an emulsifier, acceptor phase, ion pair-based extraction, and solid-phase extraction (SPE) with micellar desorption¹¹. The major beneficial properties of surfactants in the sample preparation are their good solubility and the capability to interact with analytes by various interactions such as hydrophobically, electrostatically, or combination of both. The extraction methods using surfactants

give several advantages such as being environmentally friendly, safe, low cost, and low toxicity¹¹. Therefore, surfactant is a preferable extracting solvent being used in ELLME without the necessity of a dispersant agent. The fatty acid surfactants are the suitable solvent for SFOD-ELLME because of their high freezing points and low-density (compared to water)¹⁴.

Additionally, the Association of Official Analytical Chemists (AOAC) have been encouraging the utilization of experimental design and statistical analysis on analytical quality control to improve the quality of the analytical data to determine real quantities of analytes in food and drink samples⁵. Consequently, a central composite design (CCD) was used in this research as an optimization tool based on response surface methodology (RSM) to optimize the significant independent factors that affect the method efficiency. CCD is an experimental design that is rapid and able to reduce the number of experiments for multivariate analysis¹⁵.

In this study, solidification of floating organic drop-emulsification liquid-liquid microextraction (SFOD-ELLME) coupled with digital image colorimetry (DIC) was developed. Medium-chain fatty acids were used as the extracting phase and modified paper platform digital image colorimetry with smartphone camera was used as detection method. The variables affecting SFOD-ELLME and DIC were optimized by using RSM-CCD and one factor at a time (OFAT) approach. The proposed SFOD-ELLME-DIC method was applied for the analyzing of CV and RhB in food and drink samples.

1.2 Objectives

To develop an analytical method based on surfactant-based emulsification microextraction technique coupled with digital image colorimetry on a paper platform for determination of synthetic dyes in food and drink samples.



Chapter 2 Theory and literature review

2.1 Sample preparation

Sample preparation is a part of analyzing process that mostly affects total analysis time and data quality. Sample preparation is important because even the use of an advanced instrumentation detection system cannot help to provide good data if the sample is full of interference and unsuitable to proceed in a chosen instrument. Therefore, sample preparation is still a growth trending topic of research in analytical chemistry. This step consists of all treatments such as homogenization, isolation, extraction, clean-up, and preconcentration of the analyte before the detection step to enhance the analytical capability of the analyte with a chosen measurement method¹⁶.

Nowadays, the development of a simple, cheap, rapid sample preparation is significant in many analytical methods and applications, especially for determination of trace-level of analyte from complex matrices (e.g., food, beverage, and environmental sample) that commonly need laborious steps of sample preparation. Recently, green sample preparations have been developed. Analytical chemists have paid attention to the chemical waste that is resulted from a multi-step sample preparation¹⁶. The development of green sample preparation is based on twelve principles of green chemistry, which are prevention, atom economy, less hazardous chemical synthesis, designing safer chemicals, safer solvents and auxiliaries, design for energy efficiency, use of renewable feedstock, reducing derivatives, catalysis, design for degradation, real-time analysis for pollution prevention, and inherently safer chemistry for accident prevention¹⁷.

Some traditional methods that are still acceptable and have been used until today are LLE, SPE, and solid-liquid extraction (SLE). Nevertheless, these methods have several drawbacks. LLE consumes a large amount of solvent, produces a large amount of dangerous waste, and uses harmful chemicals that can put high risk to the analyst. SPE needs synthesized materials that are somewhat expensive and difficult to synthesize and needs a long extraction time. SLE uses relatively large amount of sample and organic solvent. To overcome those drawbacks, some methods have been developed with the key concept of miniaturization, simplification, and automation¹⁶.

The miniaturization of sample preparation can be achieved also by the development of a microextraction method. The microextraction method minimizes the quantity of extracting phase (solvent or sorbent) and provides the fulfillment of several green chemistry principles, such as prevention and design for energy efficiency. The waste from the analysis process can be also prevented or minimized. Microextraction also reduces the sample preparation steps, therefore this method requires less energy than conventional sample preparation.

Recently, microextraction has gained much attention. Microextraction is divided into 2 main groups, namely solid phase microextraction (SPME) and liquid phase microextraction (LPME). SPME uses a microscale of selective sorbent. SPME provides rapid, simple, solvent-free, automatable, and easy process in many applications¹⁸. Nevertheless, SPME has several drawbacks such as instability in organic solvents, fiber damage possibility, and need for a synthetic sorbent. Therefore, the LPME seems to overcome these problems.

LPME is a method that uses a few microliters of liquid chemicals as extracting phase. Commonly, LPME uses water-immiscible solvents in small quantities. This

method can be divided into 4 main groups (Fig. 1), namely single drop microextraction (SDME), dispersive liquid-liquid microextraction (DLLME), solidification floating organic drop (SFOD), and hollow-fiber microextraction (HF-LPME)¹³. LPME has several better aspects than SPME, such as bigger extracting phase capacity, more cost effectiveness, faster phase transfer, and easier modification. DLLME appears as a rapid LPME method where the extracting phase is dispersed into small droplets with high interfacial area¹⁰ (Fig. 2). Based on Eq (1) and (2), the increasing of interfacial area (A) and total mass transfer (β^{ext}), and the decreasing of aqueous sample (V^a) can improve the LPME extraction time.

$$C^{ext}(t) = C_{eq}^{ext} (1 - e^{-kt}) \quad (1)$$

$$k = \frac{A}{V^{ext}} \beta^{ext} \left(1 + K \frac{V^{ext}}{V^a} \right) \quad (2)$$

Where,

C^{ext} is a function of microextraction time (t)

C_{eq}^{ext} is the equilibrium concentration in the extracting phase

k is rate constant

A is an interfacial area

β^{ext} is total mass transfer

V^{ext} is the volume of the extracting phase

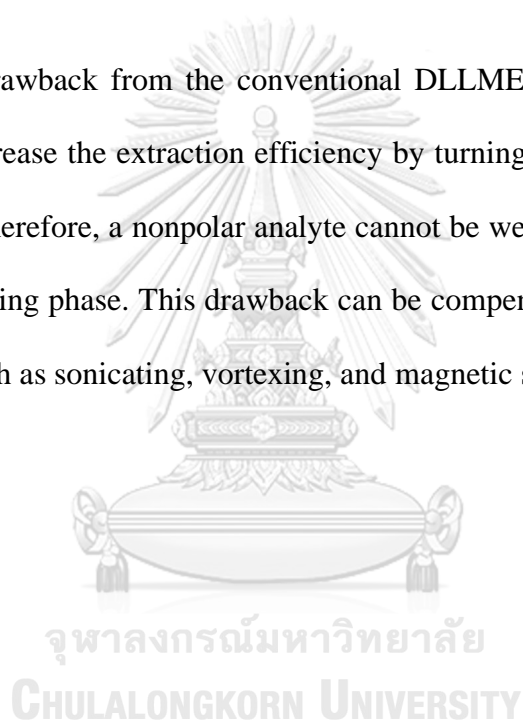
V^a is the volume of the aqueous sample

K is the distribution coefficient

DLLME is a ternary component solvent system containing extracting solvent and disperser that can be dispersed in the aqueous phase. The disperser has to be miscible both in organic extractant and aqueous sample phase¹⁹. Some disadvantages

of DLLME may be experienced; for examples, it is difficult to collect the extracting solvent that is higher density than water and some solvents are toxic and not environmentally friendly. To overcome these issues, some improvement has been developed in a newer method. SFOD-DLLME is the DLLME method that utilizes organic solvent having lower density than water that can be easily frozen or solidified and float on the top of the aqueous sample, which can be easily collected or taken out^{13, 19}.

Another drawback from the conventional DLLME is the use of a disperser. Disperser can decrease the extraction efficiency by turning the aqueous sample to be more nonpolar. Therefore, a nonpolar analyte cannot be well extracted into the water-immiscible extracting phase. This drawback can be compensated by application of an external force, such as sonicating, vortexing, and magnetic stirring²⁰.



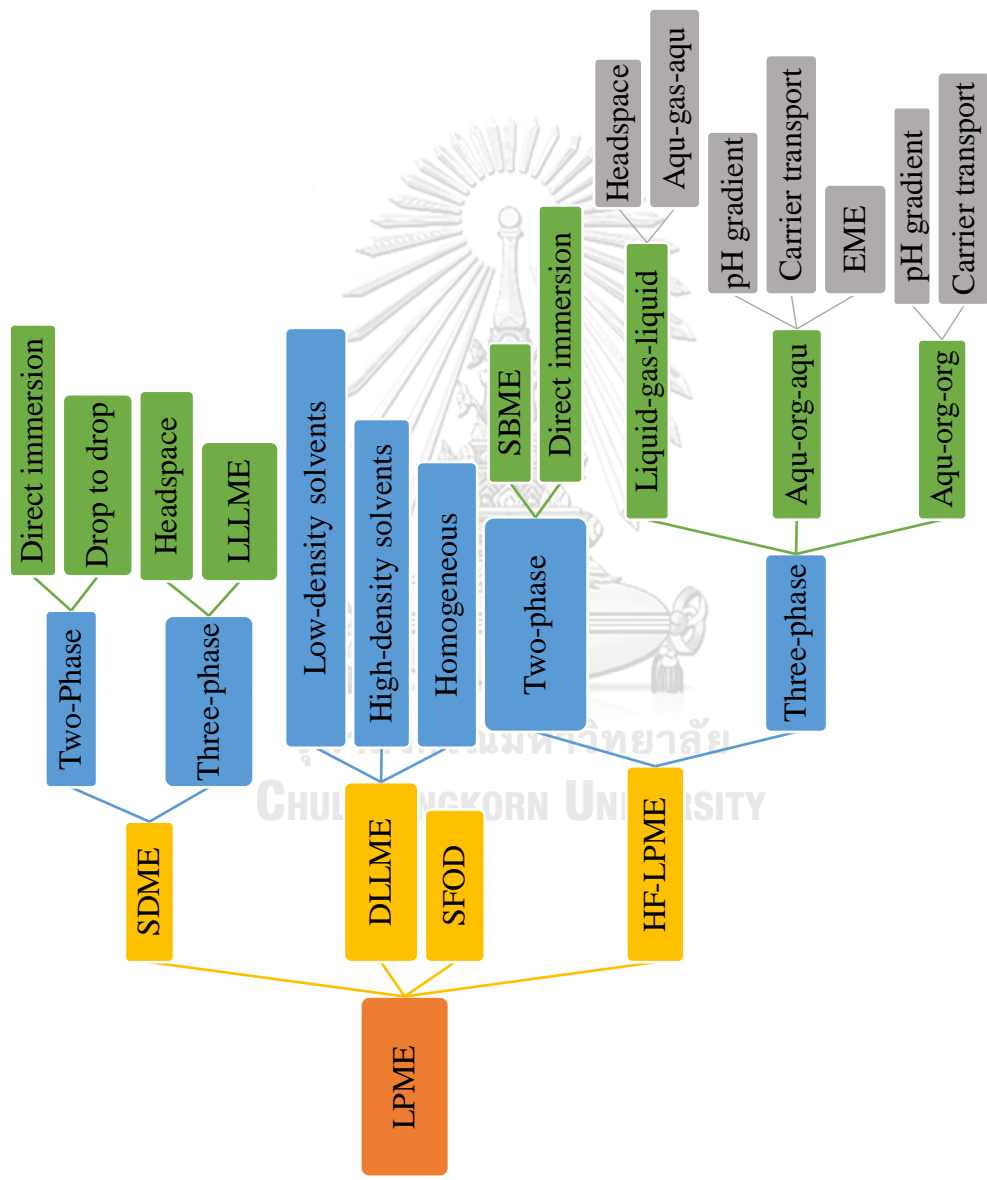


Figure 1. The classification of LPME

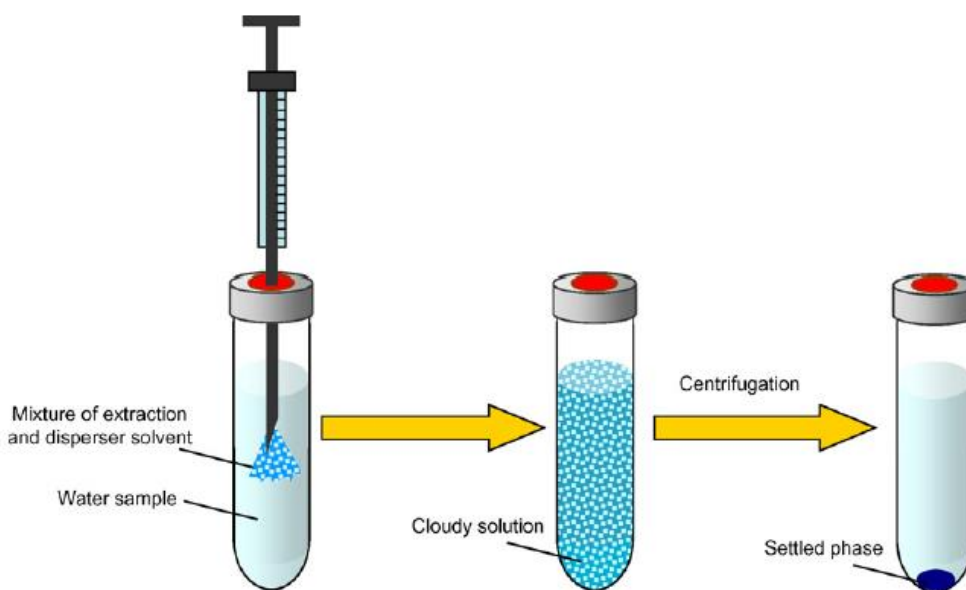


Figure 2. DLLME

For many years, the development of environmentally friendly sample preparation technique has been explored to advance this research area. The improvements could reduce or eliminate toxic and non-environmentally friendly organic solvent¹¹. The prevention of dangerous chemical waste is easier and cheaper than cleaning up waste. This prevention can be done by using a safer solvent in sample preparation. The use of fatty acid surfactant as extracting phase seems like a good tool for realization of environmentally friendly sample preparation.

2.2 Surfactant

Surfactant (surface-active agent) is an amphiphile molecule (two moieties, such as hydrophilic and hydrophobic part) (Fig. 3) that shows activity in the surface or interface of phases (Fig. 4). Nevertheless, only an equilibrated amphiphile that acts as surfactant while the over hydrophilic and hydrophobic will stay on one phase and not go to the border of two phases. The surfactants can be classified into four groups based on their head group dissociated form in water (Table 1)²¹:

- a. Nonionic surfactants are nonionized surfactants (no charge), where the polar head is a non-dissociable type, namely phenol, alcohol, amide, and ester. The nonionic surfactants commonly contain glucoside (sugar based) and polyethoxylated glycol as relatively polar head, and alkyl, alkylbenzene, and polyether chain as a lipophilic part. Around 45% of industrial surfactant is a nonionic surfactant for example: Triton, Tween, and Span.
- b. Anionic surfactants are surfactants having a negative polar (anion) head group when dissociated in water. Some anionic surfactants included in this group are fatty acid, alkyl benzene sulfonates, lignosulfonates, and sulfosuccinates. The anionic polar head usually attaches with cations, like alkaline metal (Na^+ and K^+) or quaternary ammonium. Approximately 50% of total surfactant world production is an anionic surfactant.
- c. Cationic surfactants are surfactants having a positive polar head group (cation) when dissociated in water, such as fatty amine salts and quaternary ammoniums. Its cationic polar head usually binds with anions e.g., halogen. This type is more expensive than anionic surfactants, which is caused by the utilization of a high-pressure hydrogenation reaction in the synthesizing process
- d. Amphoteric/zwitterionic surfactants are a group of surfactants having both positive and negative charges on the polar head groups when dissociated in water. Examples of this group are betaines, sulfobetaine, phospholipids, and amino acids.

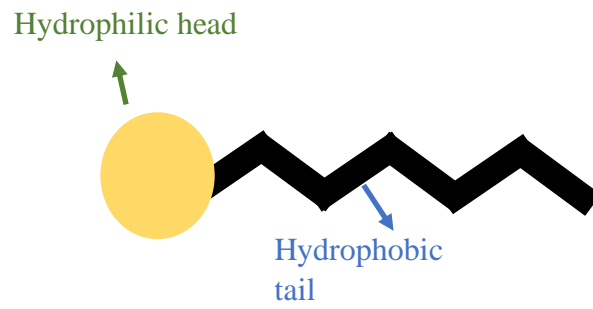


Figure 3. The general structure of surfactant

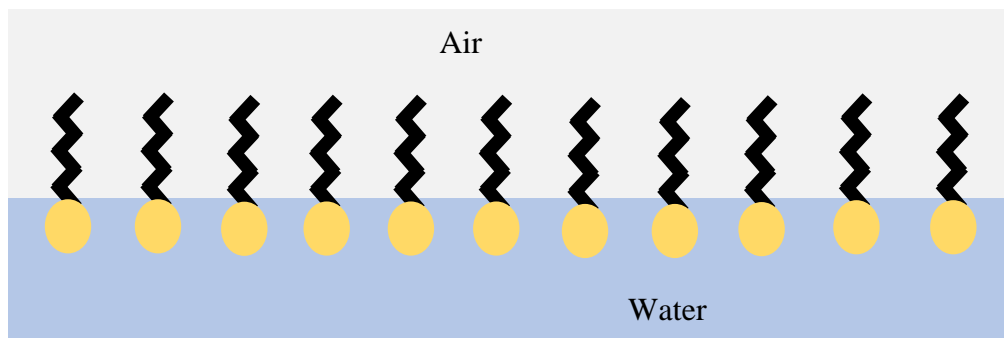
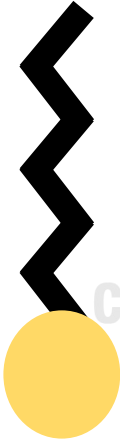
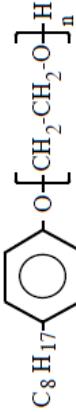

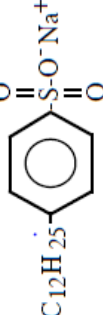

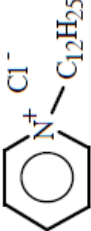




Figure 4. Surfactant line up in the water-air interface

Table 1. The type of surfactants
Types of surfactant

	Structure	Example
Nonionic surfactants		 (Polyethoxylated Octyl Phenol)
Anionic surfactants		 (Sodium Dodecyl Sulfonate)
Cationic surfactants		 (N-Dodecyl Pyridinium Chloride)
Amphoteric/zwitterionic surfactants		 (Dodecyl Betaine)

2.2.1 The roles of surfactant in sample preparation

Surfactant demonstrates excellent properties that can improve the efficiency of some sample preparation techniques, especially liquid phase extraction. There are several roles for surfactant in liquid phase extraction, such as emulsifier, extraction medium, and carrier¹¹.

Environmentally friendly surfactant as an emulsifier in the DLLME method can help to improve the green aspect and drawback of using disperser in the conventional DLLME. Surfactants as extracting phase create aggregation that can interact with analyte effectively while providing some advantages such as cost-effectiveness, less hazardousness, environmentally friendliness and low toxicity in contrast to the organic solvent. Surfactant as a carrier facilitates the specific analyte transportation through the liquid membrane or without liquid membrane¹¹. One environmentally friendly surfactant group is fatty acid^{14, 22}.

2.2.2 Fatty acid as surfactant

Fatty acids are naturally obtained or produced from various living things (e.g., marine, animal, and plant). Therefore, fatty acids can be classified as less toxic and biodegradable chemicals. Fatty acids have a carboxylic acid functional group in their polar headgroup and alkyl in their hydrophobic chain, hence fatty acid is amphiphile. When dissolved in water, the carboxylic acid functional group can be deprotonated into carboxylate group ($-\text{COO}^-$) having a negative charge, which is then categorized as anionic surfactant, accordingly. Generally, fatty acids are classified into three groups based on the aliphatic chain length, as follows^{14, 22}:

- a. Short-chain fatty acids containing less than six carbons (<C6).

- b. Medium-chain fatty acids having 6 to 12 carbons in their aliphatic group (C6-C12).
- c. Long-chain fatty acids containing 14 up to 22 carbons (C14-C22).
- d. Very long-chain fatty acids having more than 22 carbons in their aliphatic group (>C22).

The characteristics of fatty acids, such as surface activity, solubility in various solvents, and aggregation ability are determined by their structure, hydrophobic tails length, type of hydrophilic head, and the existence of additional alkyl group. Considering the properties of the medium chain, it is a good candidate for solvent in solidification surfactant-based emulsification extraction. The medium chain fatty acids e.g., hexanoic acid, pentanoic acid, octanoic acid, and decanoic acid have a relatively high freezing point, which can be easily frozen or solidified. Besides, their amphiphile properties can provide several possible intermolecular interactions with the several kinds of analyte compounds which can be effortlessly dispersed and improve the extraction efficiency¹⁴.

2.3 Digital image colorimetry (DIC)

2.3.1 Definition and principal work

Colorimetry of digital images is a method for detecting analytes based on the interpretation of color from digital images taken with a digital device and processed by a software. Some advantages that are given by this method, such as simplicity, portability, cost-effectiveness, and rapidity make it rise as the trending research topic nowadays. This method can be used for several types of analysis, such as semi-quantitative, quantitative, and cut-off analysis. Two main steps of DIC using smartphone are demonstrated in Fig. 5²³:

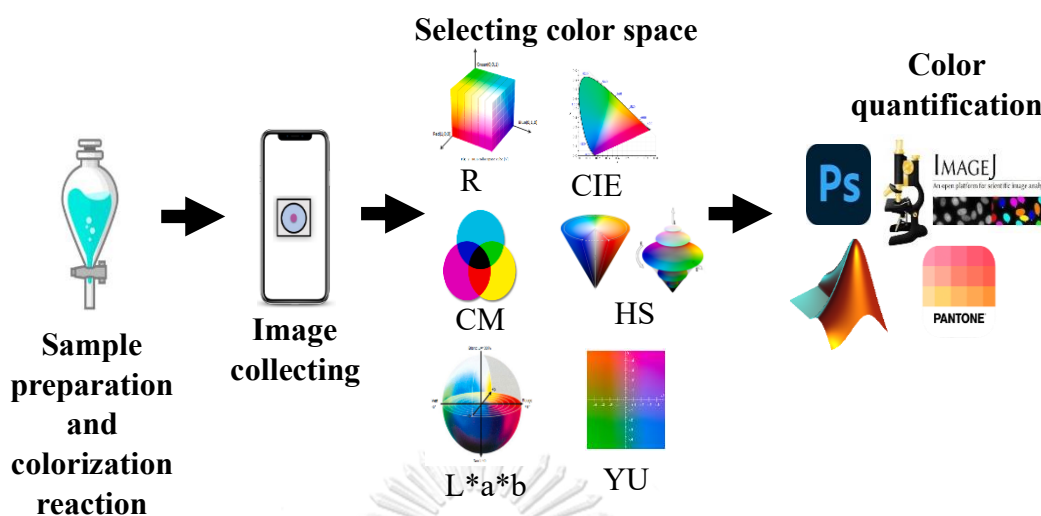


Figure 5. Procedure of smartphone digital image colorimetry

a. Image collecting

A digital device such as mobile phone camera, scanner, digital camera, and webcam is utilized to capture the image. The device captures the color and transforms the input signal into an optical and electrical signal using image sensors such as charge-coupled devices (C-CD), the contact image sensor (CIS), and complementary metal oxide semiconductors (CMOS). The quality of the image is attributed to the quality of the device, lighting condition, and the photo shooting technique.

b. Image quantitative analysis

Quantification of the image can be carried out using an image processing software, such as Image J, Adobe photoshop, Matlab, and Pantone studio with appropriate color space. In digital image colorimetry (DIC), several color spaces can be used for detection such as RGB, CMYK, HSV/HSL, CIE, XYZ, $L^*a^*b^*$, and YUV. RGB color space (0-255 range) was used in this study due to its simplicity. Generally, a color image composes of several pixels each of which consists of red, green, and blue (RGB) colors at a certain intensity ratio. The RGB color model (Fig.

6) is shown in a cube with three orthogonal coordinate axes, each of which represent the red, green, and blue colors. The axis shows the gradient of color intensity, where the diagonal line is a grey representative from black (0,0,0) to white (1,1,1). The color range usually are 0-255 (8 bit) and 0-65536 (16 bit) for each color²³.

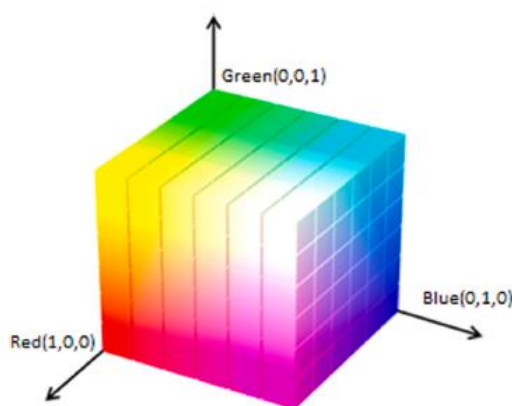


Figure 6. RGB color space cube

Digital image colorimetry has a bright prospect of developing analytical methods and devices that are simple, rapid, portable, cost-effective, and versatile which can be combined with microfluidics systems, lateral flow assays, dipstick assays, and paper-based analytical platform. This method has been developed on many analytical methods for several analytes, such as metal, heavy metal, antibiotics, herbicides, pesticides, biochemical indicators, metabolomics, and pathogens²³. Therefore, this study has the purpose to expand more of the usage of this method to analyze synthetic dyes in food and drink samples.

2.3.2 DIC method application

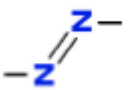
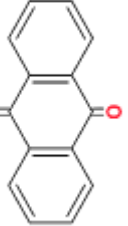
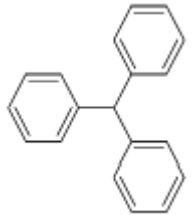
Several applications of digital image colorimetry (DIC) have been reported. A method for detection of carbaryl in food samples combined liquid phase microextraction and DIC on a microfluidic thread platform, with LOQs of 0.020-

0.027 mg/kg²⁴. Another application is the detection of total iron in water and food by coupling DLLME and DIC on a silica gel TLC plate that can maintain the color intensity for 4 hours. This method has an LOQ of 46.5 µg/L²⁵. The DIC was also applied for iron detection with a different platform, namely natural biodegradable film as an environmentally friendly substrate in DIC with an LOD of 0.09 mg/L²⁶. Apparently, one of the important parameters in DIC is the detection platform that must be stable to maintain the color intensity.

2.4 Synthetic dyes

Synthetic dyes are color substances having chromophores that can resonate and enable them to absorb visible light (400-700 nm). Chromophores are part of molecules containing unsaturated functional groups or heteroatom functional groups, such as -N=N- (azo), -NO or N-OH (nitrous), =C=O (carbonyl), and C=S (sulfur). Synthetic dyes are classified into several groups based on their chromophores, which determine their chemical and physical properties (Table 2). The color intensity of dyes and affinity in fabric are determined by auxochromes, such as -COOH (carboxyl), -NH₂ (amine), -OH (hydroxyl), and HSO₃⁻ (sulphonate)²⁷. Synthetic food colorants have been widely used in food industry to create foods more appealing and appetizing. Synthetic dyes have replaced natural colorants due to their high resistance to oxidation and high temperatures, cheaper prices, and color homogeneity²⁸.

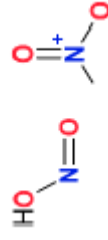
Table 2. Classification of synthetic dyes based on the type of chromophore

Classes	Chromophore structure	Example	Characteristic
Azo		Methyl orange, congo red, orange G, amaranth	The type of dyes is often used for many purposes
Anthraquinone		Remazol brilliant blue R, reactive bright blue X-BR, reactive blue 4, alizarin red S	This dyes group is the second most frequently used dyes.
Triphenylmethane		Malachite green, violet, bromophenol blue, light green SF	Triphenylmethane dyes group is mostly used in the textile industry

Nitro and Nitroso

Naphthol yellow S, disperse yellow 26, disperse yellow

The Nitro group has a hydroxyl donor group

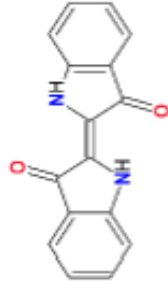


14

Indigoid

Indigo carmine and ciba blue 2B

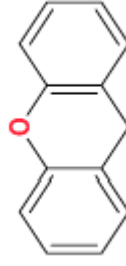
This class is used in the textile factory and is highly resistant to light and hot temperature

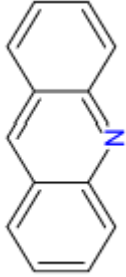


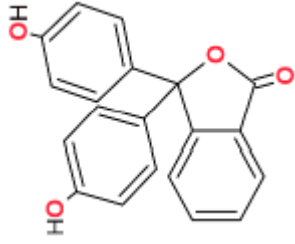
Xanthene

Rhodamine B, rhodamine 6G, rhodamine 123, fluorescein

Xanthene is a dyes class that is often used in food, ink, and cosmetics. Nevertheless, some of them are very toxic and not environmentally friendly.



Acridine

 Acridine orange and basic yellow 9
 This dyes class is resistant to a high temperature but has a low lightfastness

Phthalein

 o-cresolphthalein, thymolphthalein, dixylenolphthalein, phenolphthalein
 Phthalein dyes are water-insoluble, and alcohol-soluble. This group is used in industry, coating, and building.

The type of synthetic dyes that are often used in industry are azo, anthraquinone, indigo, xanthene, and triarylmethane. In the food industry, synthetic dyes increase appealing physical appearance in some food industries, such as beverages, candies, cereals, snacks, and desserts. Most synthetic dyes commonly used in food are anionic dyes e.g., Sunset Yellow (E-110), Ponceau 4R (E-124), Tartrazine (E-102), Solid Green FDF (E-143), and Quinoline Yellow (E-104). The type and concentration of synthetic dyes in food are being regulated in each country²⁷. Majority of synthetic dyes are harmful and hard to be degraded. They could be found in food by intentional addition to become more attractive, long-lasting food color with ease and low production cost. The addition of some synthetic dyes into the foodstuff is illegal and prohibited. Examples of illegal synthetic dyes used in food and drinks are rhodamine B and crystal violet²⁹.

2.4.1 Crystal Violet

Crystal violet (CV) is triarylmethane dye and known as basic violet 3, gentian violet, and methyl violet 10 B. CV (Fig. 7) is commonly used as an antifungal agent in aquaculture in some countries especially in developing countries because of its low cost and high efficiency. CV is a banned synthetic dye for food due to its carcinogenicity and mutagenesis in both its original form and its metabolites (leucocrystal violet). Consumption of CV has been reported to be harmful to human health³⁰.

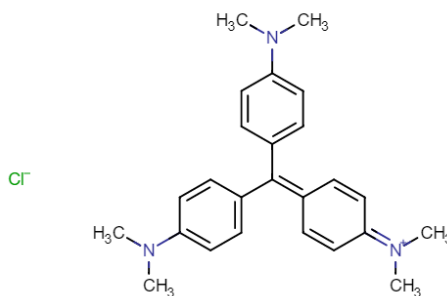


Figure 7. CV molecular structure

2.4.2 Rhodamine B

Rhodamine B (RhB) is a xanthene dye with bright pink color. RhB (Fig. 8) is a toxic xenobiotic substance and can cause several effects on the human body, such as chronic liver dysfunction or cancer and acute poisoning due to its carcinogenicity, genotoxicity, neurotoxicity, reproductive toxicity, chronic toxicity, and irritability³¹. In 1983, the Food and Drug Administration (FDA) included RhB as a carcinogen and prohibited RhB from being used in any food products³². International Agency for Research on Cancer (IARC) also classifies RhB as carcinogenic chemicals, European Food Safety Authority (EFSA) has banned RhB in food. Lethal dose 50 (LD₅₀) in rats of RhB is 89.5 mg/kg body weight based on the IARC report (1978)³³. Nonetheless, RhB is somehow still being used in food products to give them an appealing color due to its bright color, availability, and cheapness³⁴

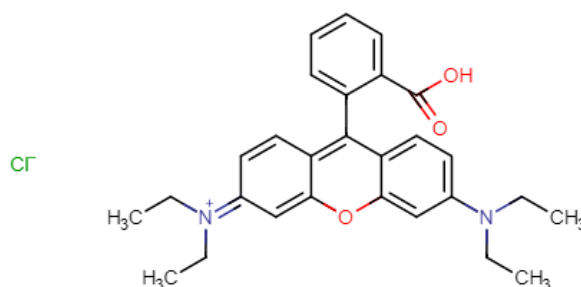


Figure 8. RhB molecular structure

2.5 RSM-CCD

RSM is a multivariable statistical method that is used to optimize the dependent variable (response) affected by several independent variables. RSM shows the correlation between parameters and response in graphical three-dimensional space and contour plots. CCD is an experimental design method that is used to construct the quadratic model in RSM³⁵. The familiar fractional factorial design utilized in the response surface model (RSM) is the central composite design (CCD). The center points in this design are supplemented with axial points (star points). Lower and higher intense values are represented by the star points (Fig. 9). The CCD model enables you to extend two level factors that are commonly used in response surface modeling and optimization³⁶.

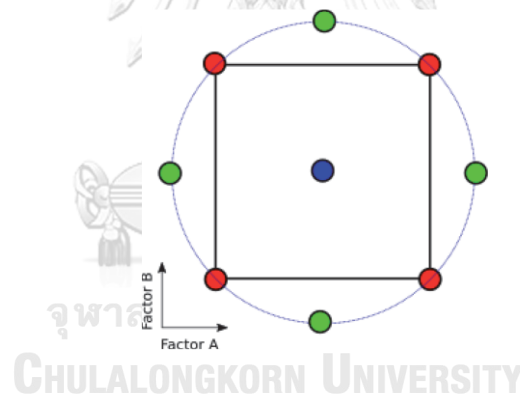


Figure 9. CCD model (green dot are star point; red dots are high and low point; blue dot is central point)

Chapter 3 Methodology

3.1 Materials and chemicals

Sodium hydroxide (NaOH), hydrochloric acid (HCl), tetrahydrofuran (C_4H_8O), crystal violet ($C_{25}N_3H_{30}Cl$) and rhodamine B ($C_{28}H_{31}ClN_2O_3$) were obtained from Merck (Germany). Octanoic acid ($C_8H_{16}O_2$) and acetonitrile (CH_3CN) were supplied from Sigma-Aldrich (United States of America). Decanoic acid ($C_{10}H_{20}O_2$) was purchased from Tokyo Chemical Industry. Sodium chloride (NaCl) was supplied from Carlo Erba Reagents (France). Filter paper grade 1 was supplied from GE Healthcare UK Limited. Milli-Q water was obtained from the water purification system Merck Millipore (United States of America), and marker (Sakura IdentitTM Pen) was used as hydrophobic barriers in paper platform.

3.2 Apparatus and software

A pH-meter from Mettler Toledo (Thailand) was used for all pH measurements. A centrifuge from Mettler Toledo (Thailand) and hot plate from Merck (Germany) were used in the extraction experiments. The built-in digital camera on a smartphone (Samsung Galaxy A52; zoom=2.5× and filter=Lolli) was used for taking digital image of the colored droplet on the paper platform for colorimetric analysis. A Puluz photo lightbox with LEDs was used to control the illumination conditions when taking the image. Mean histogram color channel was analyzed by ImageJ 1.53k (National Institutes of Health, USA). Data were analyzed by Microsoft Excel 2016 and Statgraphics centurion 18.

3.3 Fabrication of paper platform for droplet digital image colorimetry (DDIC) system

The paper platform for holding the colored droplet for digital image colorimetry was fabricated using filter paper grade 1 as illustrated in Fig. 10. A circle border (diameter of 0.7 cm, optimized diameter) was drawn on both sides of filter papers using a black hydrophobic marker ink prevent spreading of water content on the paper platform. Then, the filter paper was cut into a square shape. One side of the filter paper was covered by transparent adhesive tape to prevent the leaking of the liquid solution. A 10 μL of Milli-Q water was first dropped on the top surface of the paper platform to wet the inner circle space making the paper surface hydrophilic to maintain hemisphere shape of the colored droplet.

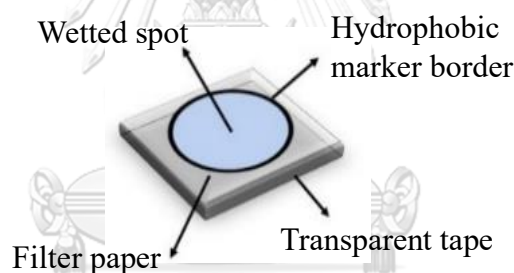


Figure 10. The paper platform for the DDIC system

3.4 SFOD-ELLME-DDIC Procedure

The sample solution was adjusted to pH 8.0 and 7.0 by 0.01 M HCl and 0.01 M NaOH for RhB and CV analysis, respectively. A 7 mL aliquot of sample solution was transferred into a centrifuge tube. Then, 21.6 μL octanoic acid was added as extracting phase to the sample solution. The mixture was manually shaken for 10 s. The cloudy solution was observed, which was a sign of emulsification. Then, the mixture was centrifuged for 5 min at 3000 rpm. The extracting phase (octanoic acid) containing the RhB or CV was separated as the top layer that adhered to the wall of

the tube. Hereafter, the solution was dipped in the ice bath to solidify the octanoic acid-rich phase for about 1 minute. Then, the sample solution was decanted. The remaining octanoic acid-rich phase was let liquefied at room temperature. The color liquid was taken and dropped on the paper platform. The color image was taken with the built-in digital camera on the smartphone inside the puluz photo lightbox (Fig. 11). Then, the color was analyzed by ImageJ software using the intensity of the red color channel (Fig. 12). The difference of red intensity (ΔI) was obtained by subtraction of each red intensity obtained from the sample or standard solution by that obtained from the blank as shown in equation (3).

$$\Delta I = |I_{\text{solution}} - I_{\text{blank}}| \quad (3)$$

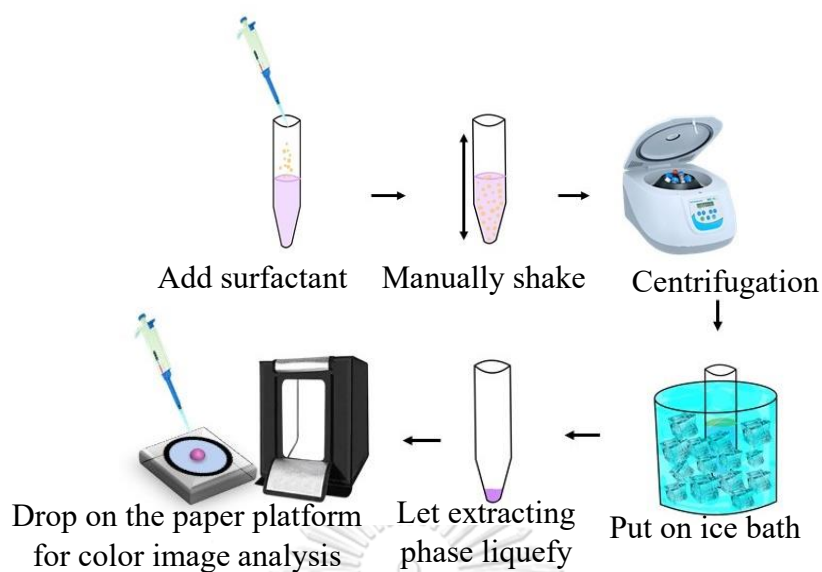
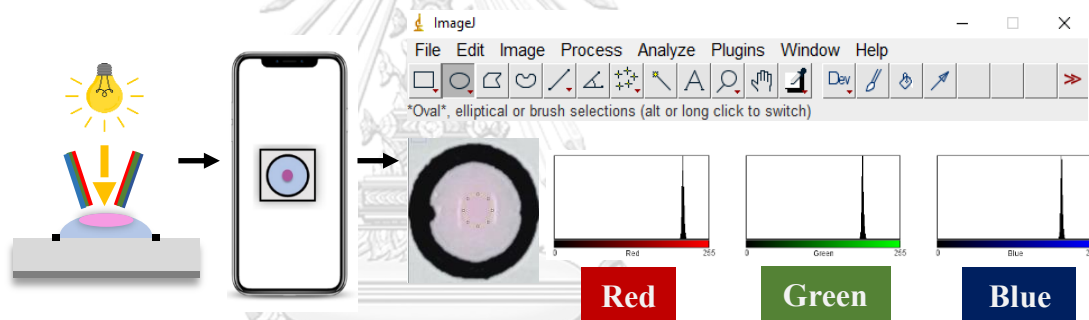


Figure 11. Schematic illustration of SFOD-ELLME-DDIC procedure



Capture picture with smartphone

Analyze color intensity with ImageJ

Figure 12. Schematic illustration of droplet digital image colorimetry (DDIC)

3.5 Experimental design

Three parameters that affect the ELLME efficiency for CV and RhB extraction were studied by RSM-CCD, including sample pH, the volume of extracting phase, and NaCl concentration. These three factors were selected based on literature reviews. Sample pH affects the form of analyte species in the sample or donor phase. The appropriate pH turns the analyte into the form that can effectively have intermolecular interaction with extracting phase molecule to increase the distribution of analyte in extracting phase. The extracting phase volume can influence the number

of intermolecular interactions with the analyte, and consequently the extraction efficiency. Salt concentrations influence the ionic strength of the solution, which affects the distribution of analyte in the organic extracting phase. These three parameters were studied by RSM-CCD. The statistical analysis was proceeded by using Statgraphics centurion 18.

This experiment was performed using DIC with a red color channel and a 7 mL solution containing 40 $\mu\text{g/L}$ of RhB and CV as a model solution for the optimization step. The sample pH was observed in the range of 4.0-10.0. Moreover, the volume of extracting phase varied in the range of 25-35 μL considering the easiness of phase separation, liquid pipetting, and the level of chemical consumption. Additionally, the studied salt concentration range was 0.08-0.32% (w/v).

3.6 Analytical performance

The analytical performance of the proposed method was assessed for linearity, LOD, LOQ, precision, accuracy, extraction efficiency, and enrichment factor. The calibration curve of 5-level concentration, 3-20 $\mu\text{g/L}$ for CV, and 10-40 $\mu\text{g/L}$ for RhB was used to determine linearity, LOD, and LOQ. Intra-day and inter-day precisions on two different concentrations for CV (15 $\mu\text{g/L}$ and 20 $\mu\text{g/L}$) and RhB (30 $\mu\text{g/L}$ and 40 $\mu\text{g/L}$) were determined. The extraction recovery (ER%) is calculated from the relationship between EF and phase ratio. The matrix effect and accuracy were expressed by the relative recovery (RR%) of spiked samples with known concentrations (for RhB: 20 $\mu\text{g/L}$ and 40 $\mu\text{g/L}$ were spiked in liquid samples and 1 $\mu\text{g/g}$ and 2 $\mu\text{g/g}$ were spiked in solid samples; for CV: 10 $\mu\text{g/L}$ and 20 $\mu\text{g/L}$ were spiked). In addition, the slope of matrix-matched calibration curves from several complex matrixes and that of calibration curve from standard solution were compared.

3.7 Sample analysis

3.7.1 Sample pre-treatment for samples of RhB

3.7.1.1 Beverage sample

Red beverage sample was purchased from a local store in Bangkok, Thailand. The beverage was diluted 50 times and adjusted to pH 8.0 prior to extraction.

3.7.1.2 Candy sample

Four different brands of candy were purchased from a local store in Bangkok, Thailand. The candy samples are pink to red color candy. Candy was grounded by mortar and pestle. A 1.0 g of grounded candy was weighed and dissolved in 50 mL of Milli-Q water. The mixture was heated to 80 °C for 20 min to facilitate the dissolution of rhodamine B in the water. Then, the dissolved candy sample was filtered by filter paper Whatman no. 1 and the pH was adjusted to pH 8.0 prior to extraction.

3.7.1.3 Jelly sample

Red jelly sample was purchased from a local store in Bangkok, Thailand. A 1.0 g of jelly was dissolved in 50 mL of boiled water. Then, the solution was filtered by filter paper Whatman no. 1 and adjusted to pH 8.0 prior to extraction.

3.7.1.4 Chili sauce

Chili sauce sample was purchased from a local store in Bangkok, Thailand. A 2.0 g of chili sauce was weighed, dissolved with 100 mL Milli-Q water, and stirred for 20 min. The mixture was filtered with Whatman filter paper no. 1 and the pH was adjusted to pH 8.0 prior to extraction.

3.7.2 Sample pre-treatment for samples of CV

3.7.2.1 Drinking water

Drinking water sample was obtained from a water purifier dispenser at Chulalongkorn university. The drinking water pH was adjusted to pH 7.0 prior to extraction.

3.8 Calculations

3.8.1 The relative recovery (RR%)

The %RR of spiked sample was calculated as the ratio of the concentration of the analyte found in the spiked samples subtracted by that in the unspiked sampled to the spiked concentration of analyte in the samples shown in equation (4).

$$RR\% = \frac{C_{\text{found}} - C_{\text{unspiked}}}{C_{\text{spiked}}} \times 100\% \quad (4)$$

Where,

C_{found} = concentration of the analyte found in the spiked sample

C_{unspiked} = concentration of the analyte in the unspiked sample

C_{spiked} = spiked concentration of the analyte in the sample

3.8.2 Enrichment factor (EF)

The EF was obtained by the ratio of the concentration of the analyte in the extracted solution to the concentration of the analyte in the sample, which can practically be observed from the signal of analyte obtained with or without microextraction system (Equation 5).

$$EF = \frac{C_{\text{extracted}}}{C_{\text{spiked}}} \quad (5)$$

Where,

$C_{\text{extracted}}$ = concentration of the analyte in the extracted solution

C_{spiked} = spiked concentration of the analyte in the sample

3.8.3 The extraction recovery (ER%)

The ER% was defined as the ratio of the mass of the analyte in the extracted solution to the mass of the analyte in the sample, which can be calculated by the relationship between EF and phase ratio shown in equation (6).

$$ER\% = \frac{n_{\text{ext}}}{n_s} \times 100\% = \frac{C_{\text{ext}}V_{\text{ext}}}{C_sV_s} \times 100\% = EF \times \frac{V_{\text{ext}}}{V_s} \times 100\% \quad (6)$$

Where,

n_{ext} = mass of the analyte in the extracting phase

n_s = mass of the analyte in the sample solution

C_{ext} = concentration of analyte in the extracting phase

C_s = concentration of analyte in the sample solution

V_{ext} = volume of the extracting phase

V_s = volume of the sample solution

3.8.4 Limit of Detection (LOD)

LOD is the lowest concentration that can be detected by the method which can be estimated based on three times of standard error of regression ($s_{y/x}$) (Equation 7).

$$LOD = \frac{3 \times \text{Standard error of the regression}}{\text{slope}} \quad (7)$$

3.8.5 Limit of Quantification (LOQ)

LOQ is the lowest concentration that can be measured with reliable accuracy which can be estimated based on ten times of standard error of regression ($s_{y/x}$) (Equation 8).

$$LOQ = \frac{10 \times \text{Standard error of the regression}}{\text{slope}} \quad (8)$$

Chapter 4 Results and discussions

4.1 Droplet digital image colorimetry

The development of a paper platform that is suitable for small volume of organic solvent is the novelty in this research. In every DIC, a suitable final solution holder platform is needed. The platform must be able to hold the final solution in one spot to maintain the color intensity. Paper platform was used in this research as the final solution holder. The paper was used due to its versatility, cheapness, modifiable, and availability. The main concept is to hold the final-colored octanoic acid-rich phase in the hemisphere shape to increase the color intensity. The glass and plastic surface were tested to hold the octanoic acid-rich phase into droplet shape, yet these materials were not suitable. Since the octanoic acid-rich phase could absorb into the paper pores causing low color intensity, making the paper surface more hydrophilic by prewetting the paper surface with water could make the paper surface more hydrophilic. The prewetting process prevents the absorption and keep the drop hemisphere shape on the top of the paper platform (Fig. 13). This treatment is simple, cheap, and might be used as an alternative approach for treating the paper surface to be more hydrophobic without using synthesized materials. Nevertheless, the obstacle from droplet shape was the light reflection that might disturb the color analysis. Therefore, the LED light source was placed on the side of the lightbox (Fig. 14) to decrease the reflection in the convex droplet surface.



Figure 13. The comparison of final solution color intensity in (a) pre-wetted paper platform and (b) normal paper platform

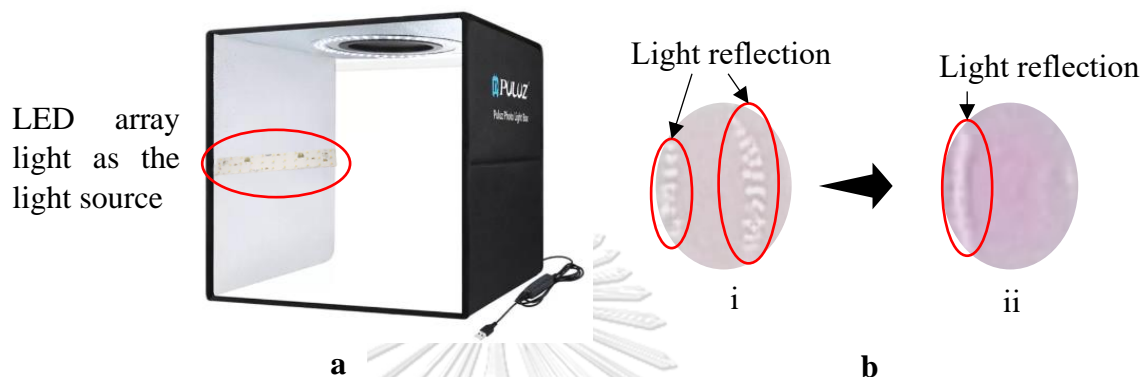


Figure 14. (a) Puluz light box setup with the light source on the side of the box (b) droplet image when the light source is on the (i) top and (ii) side of the light box

4.2 Optimization for solidification of floating organic drop-emulsification microextraction

The extraction condition of solidification of floating organic drop-emulsification microextraction using surfactant coupled with droplet digital image colorimetry (SFOD-ELLME-DDIC) was optimized by one factor at a time (OFAT) and RSM-CCD.

4.2.1 Selection of color channel

RGB color space has several color channels such as red, green, and blue channels which are important factors that can determine sensitivity in the digital colorimetry detection system. Each color channel will give different linearity and sensitivity. The chosen color channel should show the best linearity (R^2) and sensitivity (steepest slope) for the system. The RGB intensity of the extracted CV and RhB were studied in the concentration range of 20 – 60 $\mu\text{g/L}$. The intensity difference

of analyte in the extract and the blank; $\Delta I = |I_{\text{solution}} - I_{\text{blank}}|$, was determined. Fig. 15 shows the intensity difference for the red, green, and blue channel from the extraction result solution, where red channel has the highest intensity difference, highest slope, and highest R^2 for both CV and RhB.

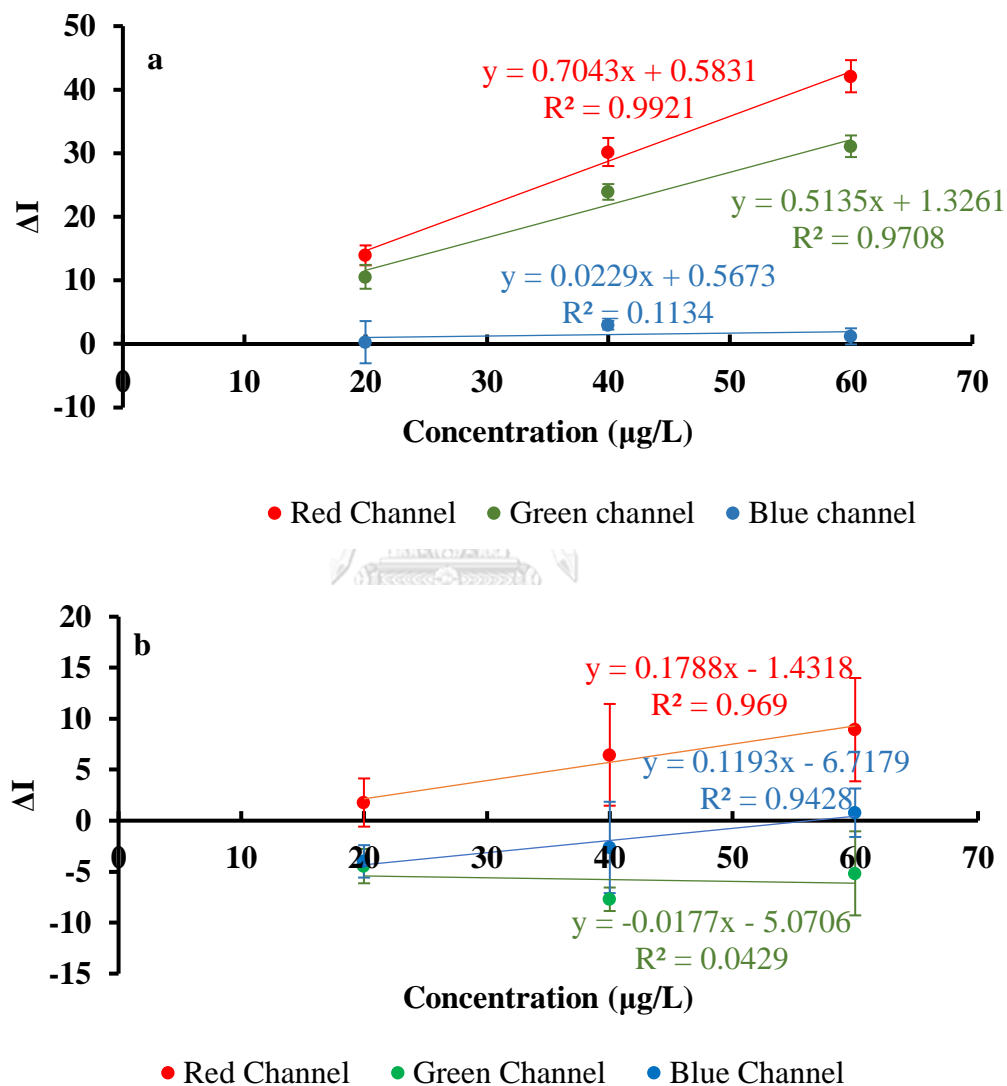


Figure 15. The red, green, and blue intensity difference of the SFOD-ELLME-DDIC of (a) CV and (b) RhB; (condition: surfactant volume, 25 μL ; pH solution, 6; agitation time, 30 s; total volume, 5 mL; centrifugation rate, 3000 rpm; centrifugation time, 10 min; distance between the camera and paper platform, 25 cm).

4.2.2 Effect of extraction solvent type

The amphiphilic medium-chain carboxylic acids have beneficial properties as extracting phases for CV and RhB. These extracting phases are faster to coalesce, easy to be emulsified, and have good intermolecular interaction with complex aromatic chemicals. In this study, two medium-chain carboxylic acids (decanoic acid and octanoic acid) were tested as extracting phase in SFOD-ELLME. The results are shown in Fig. 16.

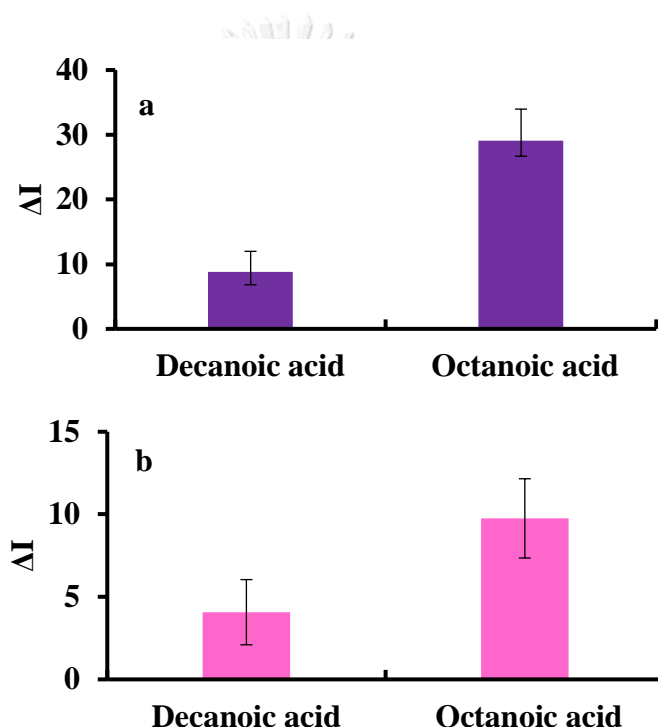


Figure 16. Effect of extraction solvent type in the SFOD-ELLME-DDIC of (a) CV and (b) RhB; (condition: surfactant volume, 25 μL ; concentration of CV and RhB, 40 $\mu\text{g/L}$; pH solution, 6; agitation time, 30 s; total volume, 5 mL; centrifugation rate, 3000 rpm; centrifugation time, 10 min; distance between the camera and paper platform, 25 cm).

As a result, octanoic acid yielded the highest ΔI of red color intensity for both CV and RhB. The reason for the result is probably because octanoic acid can undergo emulsification easier, better phase separation and easily to be liquified (freezing/melting point at 16 $^{\circ}\text{C}$)³⁷. Decanoic acid yielded lower red intensity

probably because of incomplete separation during the solidification process and dilution during the liquefaction step. Decanoic acid is a solid at room temperature (freezing/melting point at 32 °C)³⁸ and need to be dissolved by tetrahydrofuran (1 g/mL) before used. During the solidification process, decanoic acid was difficult to be separated and collected due to the presence of THF that could not be solidified (freezing/melting point at -108 °C). When the sample was decanted, some decanoic acid might be lost. Besides, during the liquefaction step, decanoic acid was redissolved in THF causing dilution effect to the color intensity measurement. Therefore, octanoic acid was chosen as the extracting solvent for further experiments.

4.2.3 Effect of manual shaking and centrifugation time

Agitation by manual shaking was used to facilitate the emulsification of extracting phase (octanoic acid) that influenced the mass transfer efficiency of the analyte. After the extraction, centrifugation was used to separate the aqueous phase and the surfactant-rich phase. In this study, shaking time ranging from 5 to 20 s and centrifugation time ranging from 3 to 20 min at 3000 rpm were varied. As shown in Fig. 17 and Fig. 18, there is no significant intensity difference observed in all range of shaking time and centrifugation time. Shaking time of 10 s and centrifugation time of 5 min were chosen for further experiments.

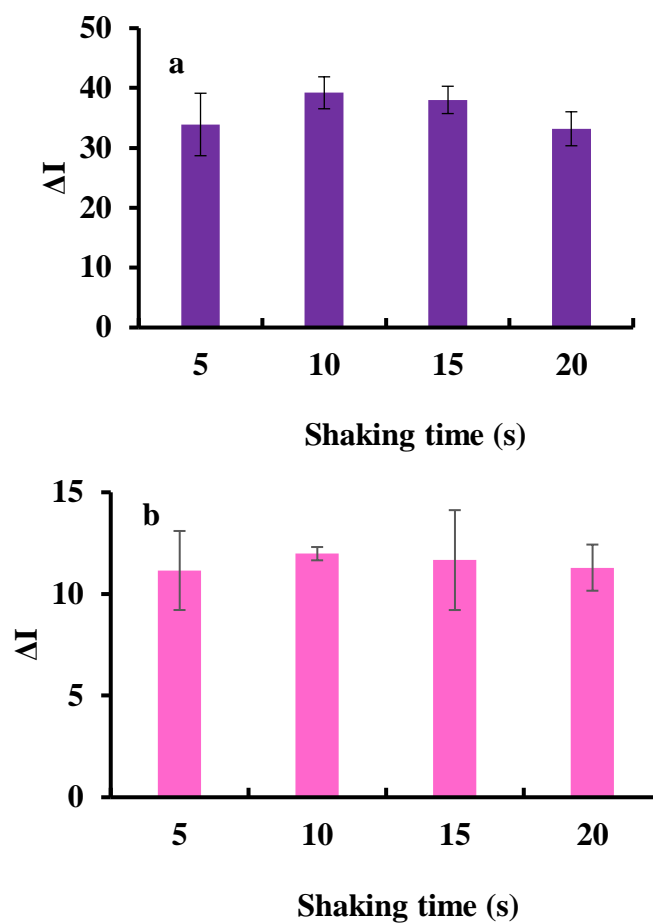


Figure 17. Effect of shaking time in the SFOD-ELLME-DDIC of (a) CV and (b) RhB; (condition: extracting phase, octanoic acid; surfactant volume, 25 μL ; concentration of CV and RhB, 40 $\mu\text{g/L}$; pH, 5; total volume, 5 mL; centrifugation rate, 3000 rpm; centrifugation time, 10 min; distance between the camera and paper platform, 25 cm).

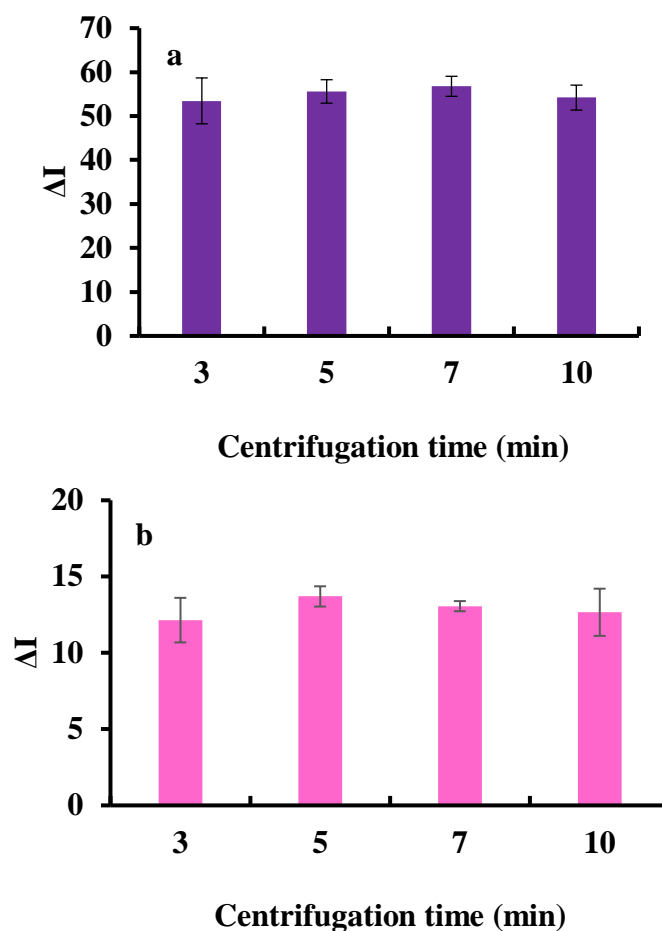


Figure 18. Effect of centrifugation time in the SFOD-ELLME-DDIC of (a) CV and (b) RhB; (condition: extracting phase, octanoic acid; surfactant volume, 25 μL ; concentration of CV and RhB, 40 $\mu\text{g/L}$; pH, 5; shaking time, 10 s; total volume, 5 mL; centrifugation rate, 3000 rpm; distance between the camera and paper platform, 25 cm).

4.2.4 Effect of sample volume

The sample volume ranging from 1 to 10 mL (the maximum volume for the centrifugation tube) were studied. As shown in Fig. 19, the intensity difference increased when the sample volume was increased up to 7 mL and not significantly increased for the sample volume of more than 7 mL. The increased sample volume would provide more mass of analyte to be transferred into the extracting phase; however, at one point the mass extracted could have been limited by the capacity of

the extracting solvent. The sample volume of 7 mL was chosen for the next experiment.

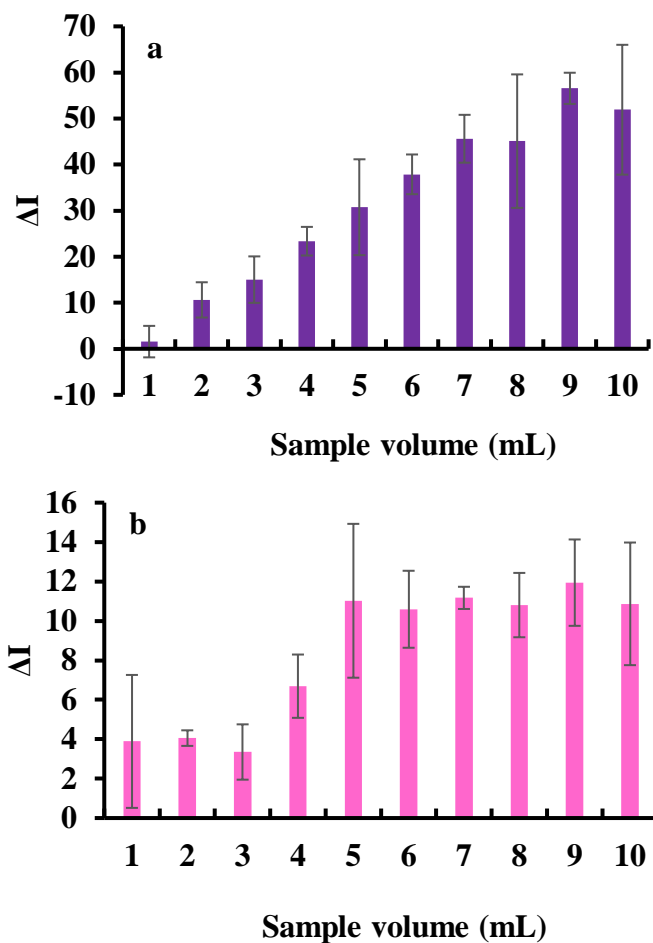


Figure 19. Effect of sample volume in the SFOD-ELLME-DDIC of (a) CV and (b) RhB; (condition: extracting phase, octanoic acid; centrifugation rate, 3000 rpm; surfactant volume, 25 μL ; concentration of CV and RhB, 40 $\mu\text{g/L}$; pH solution, 6; shaking time, 10 s; centrifugation rate, 3000 rpm; centrifugation time, 5 min; distance between the camera and paper platform, 36 cm).

4.2.5 Optimization of camera-paper platform distance

The optimization of distance will provide the best configuration that can give the best color intensity as the result of color reflection. In this study, 3 distance values were tested, including 36 (maximum height of the lightbox), 25, 14 cm. As shown in Fig. 20, the best distance was 36 cm, probably because this distance gave the best

efficiency of autofocus to obtain optimum sharpness³⁹. Hence, 36 cm was used for the next experiments.

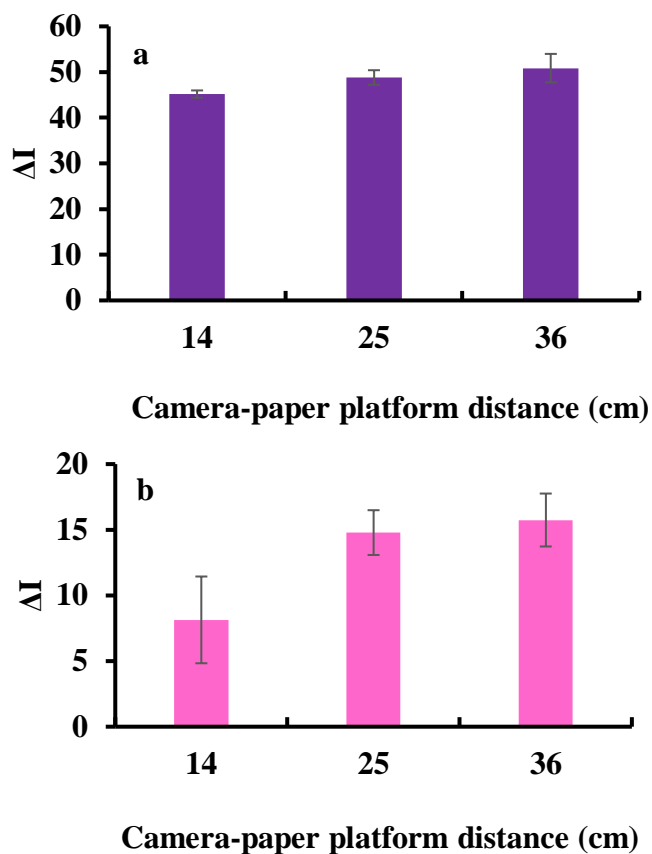


Figure 20. Optimization of camera-paper platform distance in the SFOD-ELLME-DDIC of (a) CV and (b) RhB; (condition: extracting phase, octanoic acid; surfactant volume, 25 μ L; concentration of CV and RhB, 40 μ g/L; pH, 5; shaking time, 10 s; total volume, 5 mL; centrifugation rate, 3000 rpm, centrifugation time, 5 min).

4.2.6 Experimental design

In the CCD, three factors such as sample pH (A), the volume of extracting phase (B), and NaCl concentration (C) were studied using 5 levels ($-\alpha$, -1, 0, +1, $+\alpha$) and two replicates of the central point (Table 7). Therefore, 17 runs were performed in total with a certain experimental design level of factors that were randomly chosen by Statgraphics centurion 18 and the color intensity (ΔI) was measured (Table 8).

The ANOVA table (Table 9) and Pareto chart (Fig. 21) show the statistical significance of each parameter by comparing the mean square against an estimate of

the experimental error. In Fig. 21, gray bars in the Pareto chart indicate positive correlation to the response intensity for the SFOD-ELLME-DDIC (changes are in the same direction) and blue bars indicate negative correlation (changes are in the opposite direction). The vertical line presents the threshold of significant level at 95% confidence. The bar that passes this threshold suggesting the significant effect to the response intensity (P-value < 0.05). The parameters that give negative correlation to the response color intensity are extracting phase and salt concentration for both CV and RhB. Sample pH shows negative correlation in extraction of CV while gives positive correlation in extraction of RhB. Only quadratic term of pH (AA) in CV optimization has significant effect to the response intensity (P-value < 0.05) indicating that the proposed method is robust in that range of parameters.

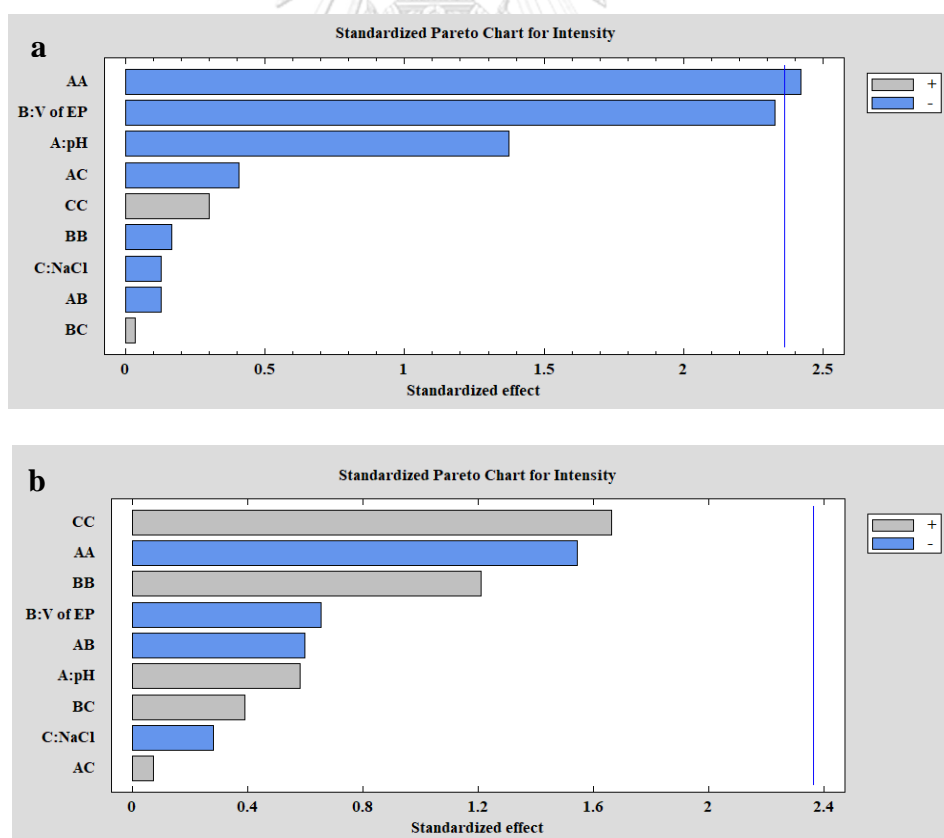
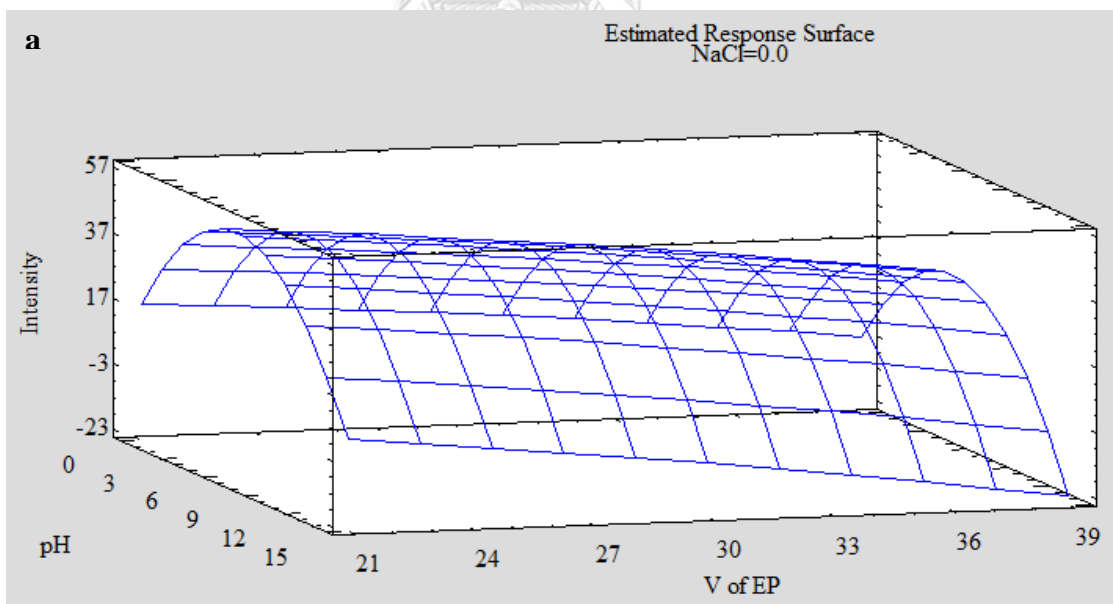


Figure 21. Pareto Chart of several affecting independent variable for (a) crystal violet and (b) rhodamine B

The three-dimensional illustration of the response surface is shown in Fig. 22. The optimum level of sample pH was 7.0 for CV and 8.0 for RhB, where both CV and RhB exists in its less polar form and more lipophilicity and tends to distribute more in the octanoic acid. At $\text{pH} < 7$, CV (pK_a 4.83) and RhB ($\text{pK}_a = 3.50$ and 4.34) were protonated and dominated as charged species (Fig 26a and Fig. 27) which showed less distribution in the organic solvent (Fig. 26b and Fig. 28). Therefore, low extraction efficiency or low color intensity was observed. At higher pH, the phase separation became difficult, hardly separated, and collected, probably because the octanoic acid started to be dissociated. Besides, the collected extracting phase could not form hemisphere shape on the paper platform resulting in no intensity could be measured (pH 12 in Table 8).



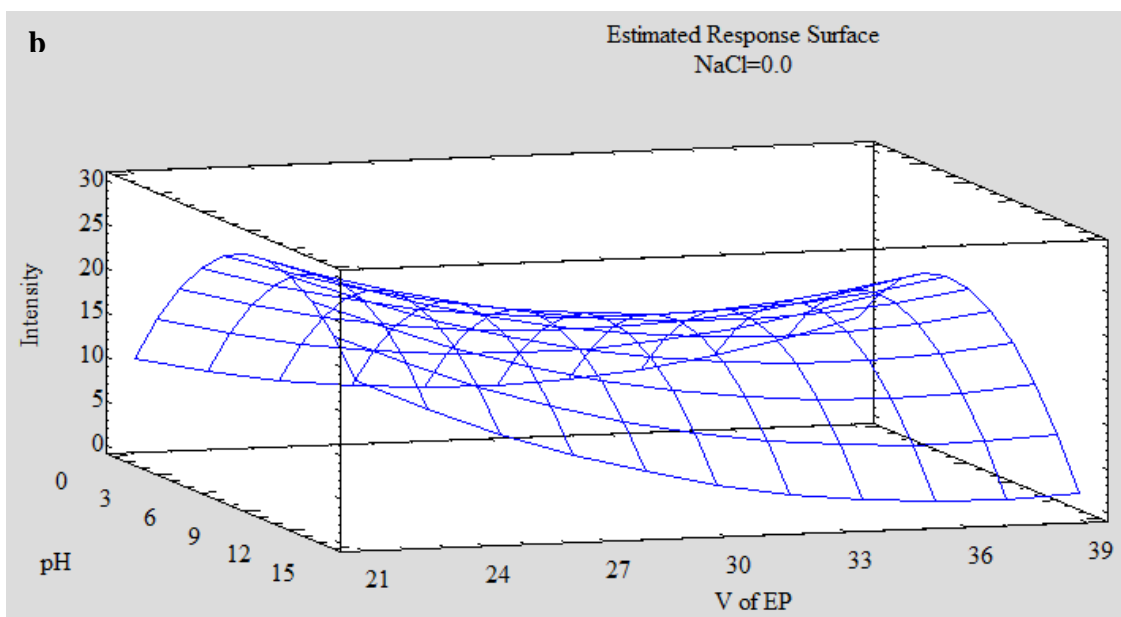


Figure 22. Response surface of sample pH and volume of extracting phase; **(a)** CV and **(b)** RhB

Increase in extracting phase volume up to 21.6 μL could improve the extraction efficiency and response intensity. Moreover, the more extracting phase volume could lead to analyte dilution and decrease in response intensity. Salt concentration shows a negative correlation to color intensity (Fig. 21). It seems that salt may have electrostatic interaction with polar moiety of the surfactant molecule that could affect the mass transfer of the analytes (CV and RhB) in the extracting phase.

4.2.7 The effect of the region of interest (ROI) area in DIC analysis

The region of interest (ROI) is the feature of ImageJ software that allows the specific area to be selected for color analysis. The ROI was optimized by measuring the red intensity (R) on the drop area ranging of 100-2000 px^2 using an elliptical selection toolbar. As shown in Fig. 23, the red color intensity observed in all areas of the drop was not significantly different based one-way ANOVA results shown in

Table 10 (P-value > 0.05) for both RhB and CV. Therefore, the red intensity could be measured on the drop regardless of the ROI area.

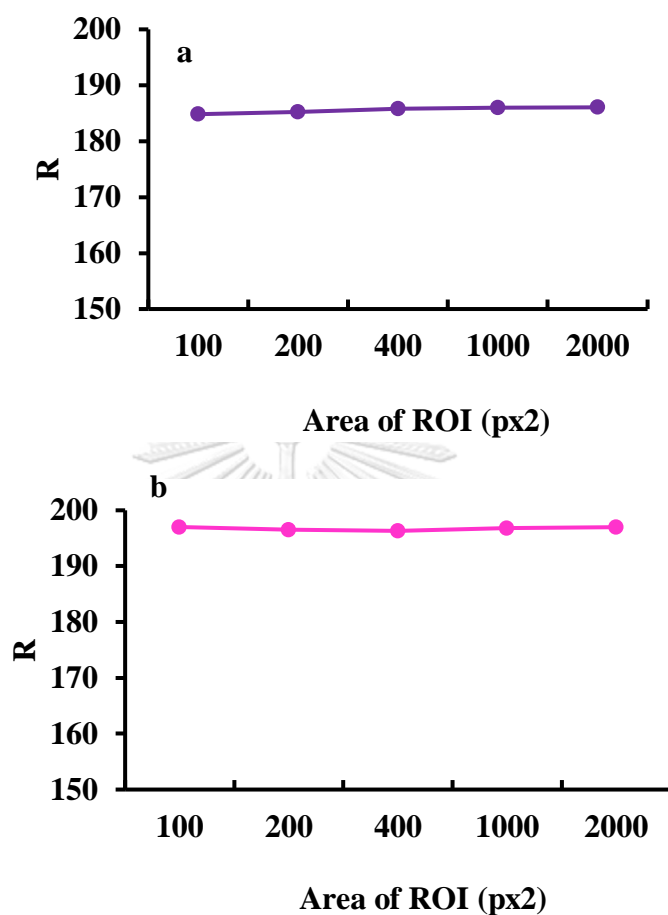


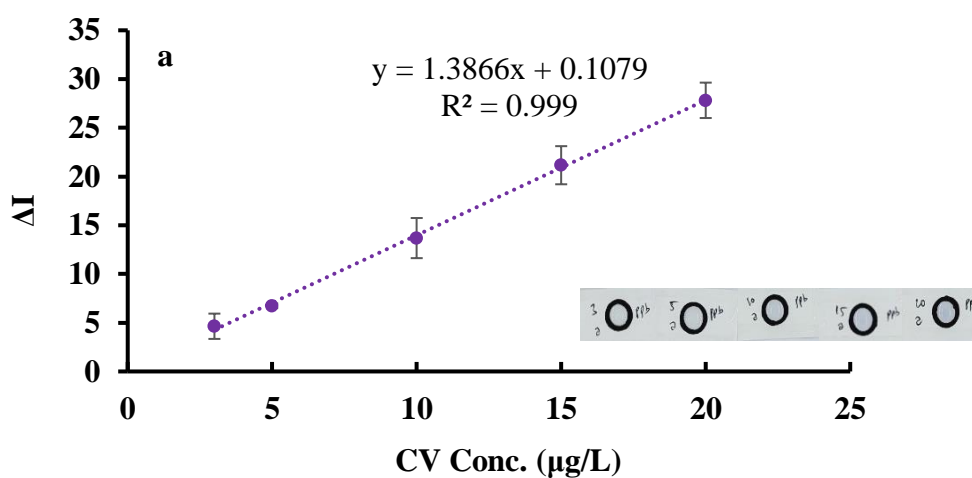
Figure 23. The effect of ROI area in the SFOD-ELLME-DDIC of (a) CV and (b) RhB; (condition: surfactant volume, 21.6 μL ; concentration of RhB, 40 $\mu\text{g/L}$; concentration of CV, 20 $\mu\text{g/L}$; pH, 8; shaking time, 10 s; total volume, 7 mL; centrifugation rate, 3000 rpm; centrifugation time, 5 min; distance between the camera and paper platform, 36 cm).

In summary, the optimum extraction conditions for SFOD-ELLME of CV and RhB can be described as that a sample of 7 mL adjusted to pH 7.0 for CV and pH 8.0 for RhB was extracted with 21.6 μL of octanoic acid shaken for 10 s and centrifuged for 5 min at 3000 rpm for phase separation without adding salt. Then, the extracted drop was removed and dropped on the paper platform for taking a digital image at the

distance of 36 cm in the light-controlled box. The color image of the drop was analyzed at the red intensity.

4.3 Analytical features

Analytical performance of the SFOD-ELLME-DDIC of CV and RhB that was summarized in Table 3. Fig. 24 displays the calibration curves of CV and RhB showing good linear relationship for the concentrations range of 3-20 $\mu\text{g/L}$ for CV and 10-40 $\mu\text{g/L}$ for RhB with R^2 greater than 0.995. The limit of detection (LOD) and limit of quantitation (LOQ) were determined based on 3 times and 10 times standard error of the regression line ($S_{y/x}$). The LOD and LOQ for CV were 0.8 $\mu\text{g/L}$ and 3 $\mu\text{g/L}$ and for RhB were 3 $\mu\text{g/L}$ and 10 $\mu\text{g/L}$, respectively. The enrichment factors (EF) were 288 and 97 for CV and RhB, respectively. The intra-day and inter-day precision reported as relative standard deviation (%RSD) at the concentration of CV and RhB were less than 14% RSD, respectively. The extraction recovery (ER%) calculated using the relationship of EF and the volume ratio was 89% for CV and 30% for RhB. According to the AOAC guideline, all the parameters are acceptable.



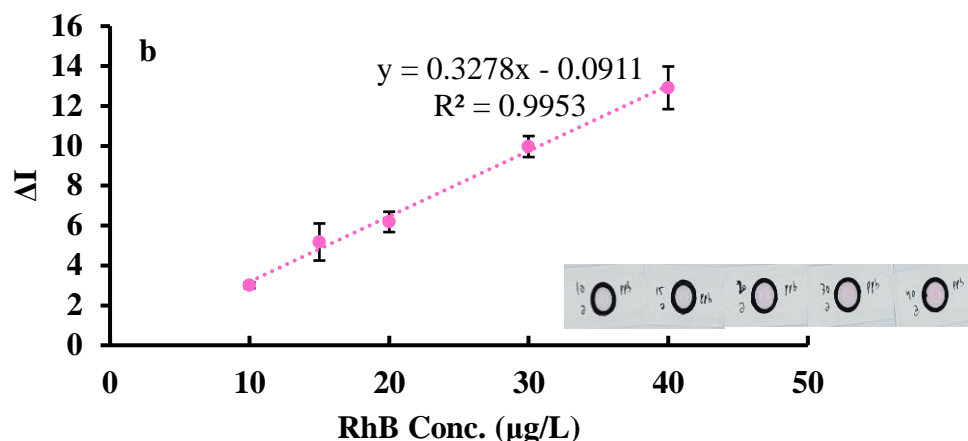


Figure 24. Calibration curve (a) CV 3-20 $\mu\text{g/L}$ and (b) RhB 10-40 $\mu\text{g/L}$ with (condition: sample volume, 7 mL; pH of sample, 7.0 for CV and 8.0 for RhB; extracting phase (octanoic acid) volume, 21.6 μL ; shaking time, 10 s; centrifugation time, 5 min; centrifugation rate, 3000 rpm; distance between the camera and paper platform, 36 cm)

Table 3. Analytical figures of merit of the developed SFOD-ELLME-DDIC procedure.

Parameters	CV		RhB	
Linear range	3-20 $\mu\text{g/L}$		10-40 $\mu\text{g/L}$	
LOD ^a	0.8 $\mu\text{g/L}$		3 $\mu\text{g/L}$	
LOQ ^b	3 $\mu\text{g/L}$		10 $\mu\text{g/L}$	
Linearity (R^2)	0.999		0.995	
Intra-day precision, RSD% ^c (n = 3)	15 $\mu\text{g/L}$	7%	30 $\mu\text{g/L}$	5%
	20 $\mu\text{g/L}$	4%	40 $\mu\text{g/L}$	8%
Inter-day precision, RSD% (n = 3 \times 3)	15 $\mu\text{g/L}$	7-10 %	30 $\mu\text{g/L}$	5-8%
	20 $\mu\text{g/L}$	3-7 %	40 $\mu\text{g/L}$	8-14%
ER% ^d	89%		30%	
EF ^e	288		97	

^a Limit of detection

^b Limit of quantification

^c Relative standard deviation

^d Extraction recovery

^e Enrichment factor

4.4 Matrix effect analysis

For determination of RhB, samples containing red color such as berry flavored beverage, candy, jelly, and chili sauce were chosen for possible matrix effect or matrix interference study. The berry flavored beverage sample had red color, which was too intense for the analysis. Therefore, the beverage was diluted 50 times prior to

extraction. The matrix effect was evaluated by comparison of the slopes from the matrix-matched calibration curve and the external standard calibration curve shown in Fig. 25. Most of the samples gave the slopes similarly to that of the standard solution indicating that matrix effect was not significant. According to the information listed on the packaging (Table 11), the red color samples commonly contain coloring agents such as Allura red AC (INS 129), Ponceau 4R (INS 124), tartrazine, betanin, and anthocyanin peonidin-3-O-galactoside. Those dyes are classified as synthetic and natural dyes that have low lipophilicity. Therefore, those dyes might not be extracted by octanoic acid and interfere the system. The slope of chili sauce was much deviated from the slope of the standard solution suggesting that there was possible matrix effect. Apparently, the matrix of the chili sauce contains yellow color background, which might be capsanthin⁴⁰, a natural antioxidant commonly found in chili. Capsanthin is an alkaloid group chemical with 11 conjugated double bonds, hydroxyl, a conjugated keto group, and cyclopentane, which would be present in neutral form with high lipophilicity in any pH range (Fig. 29). This color substance could have been co-extracted into octanoic acid and subsequently affected the measurement of the red intensity. Therefore, for chili sauce, the matrix-matched calibration curve is used.

The method was attempted to extract and determine RhB in chili powder samples, but it was not successful. As similarly observed in the chili sauce sample, chili powder contains some chemicals mainly Capsanthin that can be extracted into the octanoic acid and disturb the colorimetric detection system. As shown in Fig. 30, the chili powder that was extracted by ethanol and let dry contained red-orange color oily residue assumed as capsanthin⁴⁰ at the bottom of the beaker. To avoid the

extraction of hydrophilic capsanthin, the chili powder was first extracted with water and then extracted with octanoic acid. As shown in Fig 31, the extract still contained red-orange color that strongly interfere with the digital image colorimetry. Besides, some oily substances could disturb the coalescence in the phase separation step. Therefore, this developed method cannot be applied to chili powder. This method is successfully applied to chili sauce because it contains lower amount of chili composition and less amount of capsanthin.

For determination of CV, natural water samples such as river water were chosen for study. River waters contain solid suspensions that may be from sand, humus, and microplastic (Fig. 32). Therefore, the sample was filtered prior to extraction. Experimentally, no CV was found in the extracted spiked river water samples (Fig. 33). Since CV was spiked into the sample prior to filtration, CV could have been absorbed onto the suspended organic matters and could be filtered out with particulate matters⁴¹. To prove this hypothesis, CV was spiked into the sample after removal of particulate matters and then extracted. As shown in Fig 34, CV was found.

This developed method may have failed to apply for determination of CV in fish tissue samples. Fish tissue contains proteins that can have hydrophobic intermolecular interaction with CV⁴² that could cause difficulty in extraction of CV in fish tissue. Acetonitrile was exploited as an extracting solvent of CV in fish tissue. Acetonitrile is a solvent commonly used for protein denaturation or protein precipitation⁴³. Despite the protein structures have been disrupted and precipitated and CV has been released, CV could still be absorbed on the protein precipitation (Fig. 35) and could be lost when filtered.

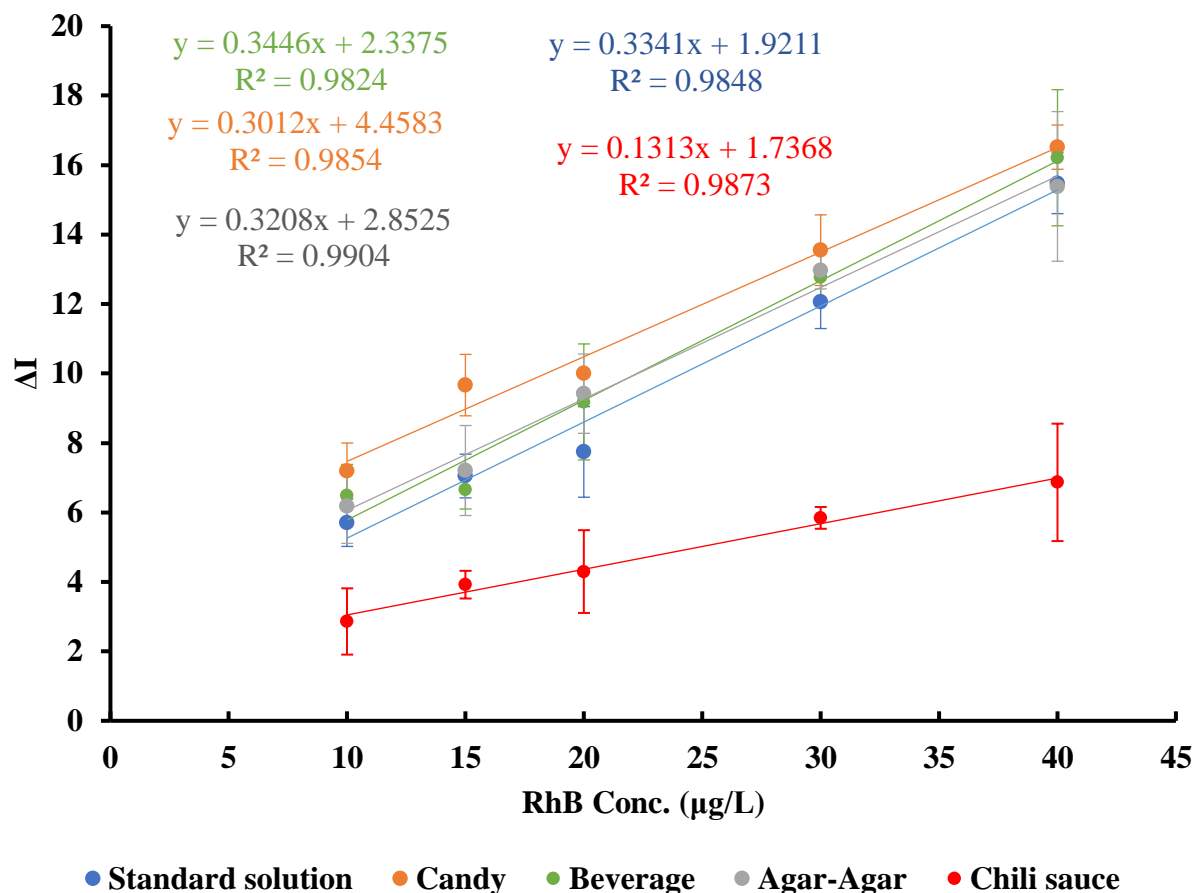


Figure 25. Matrix-matched calibration curve of real samples and external calibration curve of standard solution.

4.5 Analysis of real samples

The method of SFOD-ELLME-DDIC was applied for determination of spiked RhB in various samples. The results are summarized in Table 4. The relative recoveries (%RR) of spiked RhB at 20 μg/L and 40 μg/L in beverage, candy and jelly samples were in the range of 95-102 %; 73-113 %; and 87-110 %, respectively. The RR% of spiked RhB at 1 μg/g and 2 μg/g in the chili sauce sample were in the range of 93-98 % using matrix-matched calibration curve. The RSD% of less than 17 % was obtained for all samples. This method was applied for determination of spiked CV in drinking water. The results are summarized in Table 5. The %RR of spiked CV at 10 μg/L and 20 μg/L in drinking water were in the range of 104 % and 113 %.

Table 4. Determinations of RhB in several samples by SFOD-ELLME-DDIC (n=3)

Sample	Added ($\mu\text{g/L}$)	Found ($\mu\text{g/L}$)	RR (%)	RSD (%)
Beverage	0	n.d.	-	-
	20	20.4	102	17
	40	38.0	95	5
Candy 1	0	n.d.	-	-
	20	21.2	106	18
	40	39.5	99	11
Candy 2 (no.4)	0	n.d.	-	-
	20	21.9	110	14
	40	30.1	75	10
Candy 3 (no. 5)	0	n.d.	-	-
	20	20.3	102	3
	40	29.2	73	12
Candy 4 (no. 6)	0	n.d.	-	-
	20	22.6	113	1
	40	34.2	86	2
Jelly	0	n.d.	-	-
	20	22.0	110	10
	40	34.6	87	7
Sample	Added ($\mu\text{g/g}$)	Found ($\mu\text{g/g}$)	RR (%)	RSD (%)
Chili sauce	0	n.d.	-	-
	1	0.9	95	15
	2	1.9	98	12

Table 5. Determinations of CV in drinking water sample by SFOD-ELLME-DDIC (n=3)

Sample	Added ($\mu\text{g/L}$)	Found ($\mu\text{g/L}$)	RR (%)	RSD (%)
Drinking water	0	-	-	-
	10	10.4	104	6
	20	22.6	113	11

4.6 Significance and implications

This developed method combines the SFOD-ELLME and DIC. This combination provides a high enrichment factor from the ELLME that can serve as a good sensitivity and simple detection method for the DIC system. From previous research studies (Table 6), the development of a tandem method between LPME and DIC for synthetic dye determination has still not been developed. Therefore, this aspect is one of the novelties of this research.

Table 6. Several analytical methods for synthetic dyes analysis

Analyte	Sample preparation method	Detection method	Matrix	LOD	LOQ	RSD (%)	RR (%)	Sample preparation time	Volume of extracting phase (μL)	Ref
RhB	Flow injection-Surfactant mediated extraction	Fluorescence	Paprika, chimi churri, rice spice, pizza spice	$0.12 \mu\text{g L}^{-1}$	$0.40 \mu\text{g L}^{-1}$	-	95.3-118.9%	50 samples per hour	2000	44
MG and CV	magnetic solid-phase extraction (MSPE)	ultra-high-performance liquid chromatography-tandem mass spectrometry	Fish	MG: 0.30 ng/mL and CV: 0.08 ng/mL	MG: 1.00 ng/mL and CV: 0.25 ng/mL	< 4.37%	83.15%-96.53%	60 min	2000	45
RhB	Solid-liquid extraction	Surface-enhanced Raman spectroscopy (SERS)	Chili powder	10^{-6} g g^{-1} for chili powder ($5 \times 10^{-7} \text{ g mL}^{-1}$ in extraction agent)	-	< 5%	96.4%-108.9%	Integration time = 5s	2000	34

Chapter 5 Conclusion

This research has successfully developed the extraction method based on ELLME coupled with DIC for determination of synthetic dyes such as rhodamine B and crystal violet in various complex food and drink samples. The use of fatty acid surfactant as the extracting solvent provides microextraction via emulsification yielding high enrichment factor without assistance of disperser solvent. The extracted phase could be easily separated and collected by solidification approach at low temperature. The extracted droplet is then defrosted and dropped on the paper platform for rapid and simple DIC detection. The method is applied for determination of spiked CV and RhB in food samples showing good %RR and %RSD with LOQ at 3 and 10 ug/L for CV and RhB, respectively. However, this developed method may have some limitations for samples containing lipophilic components whose color could interfere with DIC method and those containing absorptive particle that could affect extraction efficiency. By using surfactant as extracting phase with very small volume and paper platform, this method can be considered green analytical method, which complies to green chemistry principles.

APPENDIX

Table 7. The experimental levels of the variable in the CCD

Variable parameter		Variable levels ($\alpha=1.68$)				
		- α (low)	-1	0	+1	+ α (high)
A	Sample pH	2.0	4.0	7.0	10	12
B	Volume of extracting phase (μL)	21.6	25	30	35	38.4
C	NaCl concentration (m/v%)	0	0.1	0.2	0.3	0.4

Table 8. The runs of CCD and the measured intensity of CV and RhB.

Run	A	B	C	$^a\Delta I_1$	$^a\Delta I_2$
1	7.0	30.0	0.4	37.3	17.1
2	10.0	25.0	0.3	40.8	18.2
3	12.0	30.0	0.2	0	0
4	4.0	25.0	0.3	40.6	7.2
5	7.0	30.0	0.0	34.6	16.1
6	4.0	25.0	0.1	41.3	13.1
7	10.0	35.0	0.3	27.2	14.2
8	7.0	30.0	0.2	37.4	12.6
9	4.0	35.0	0.1	28.9	10.4
10	7.0	30.0	0.2	37.1	9.2
11	7.0	21.6	0.2	41.2	17.5
12	7.0	38.4	0.2	23.5	12.3
13	10.0	25.0	0.1	45.0	18.1
14	2.0	30.0	0.2	30.1	8.5
15	10.0	35.0	0.1	32.6	17.1
16	7.0	30.0	0.2	42.9	12.3
17	4.0	35.0	0.3	30.4	12.6

^a ΔI is the difference between color intensity of standard solution from blank; 1 and 2 refer to CV and RhB

Table 9. Analysis of Variance (ANOVA) of CCD

Source	Sum of Squares		Df	Mean Square		F-Ratio		P-Value	
	CV	RhB		CV	RhB	CV	RhB	CV	RhB
A: sample pH	156.398	7.06061	1	156.398	7.06061	1.89	0.34	0.2120	0.5790
B: V of EP	450.049	8.887	1	450.049	8.887	5.43	0.43	0.0526	0.5348
C: NaCl concentration	1.34748	1.6371	1	1.34748	1.6371	0.02	0.08	0.9021	0.7875
AA	486.233	49.8188	1	486.233	49.8188	5.86	2.39	0.0460	0.1662
AB	1.31058	7.50001	1	1.31058	7.50001	0.02	0.36	0.9035	0.5677
AC	13.6608	0.103961	1	13.6608	0.103961	0.16	0.00	0.6969	0.9457
BB	2.22116	30.5917	1	2.22116	30.5917	0.03	1.47	0.8746	0.2652
BC	0.091592	3.14249	1	0.091592	3.14249	0.00	0.15	0.9744	0.7095
CC	7.39997	57.6622	1	7.39997	57.6622	0.09	2.76	0.7738	0.1404
Total error	580.455	146.03	7	82.9222	20.8614				
Total (corr.)	1792.82	360.625	16						

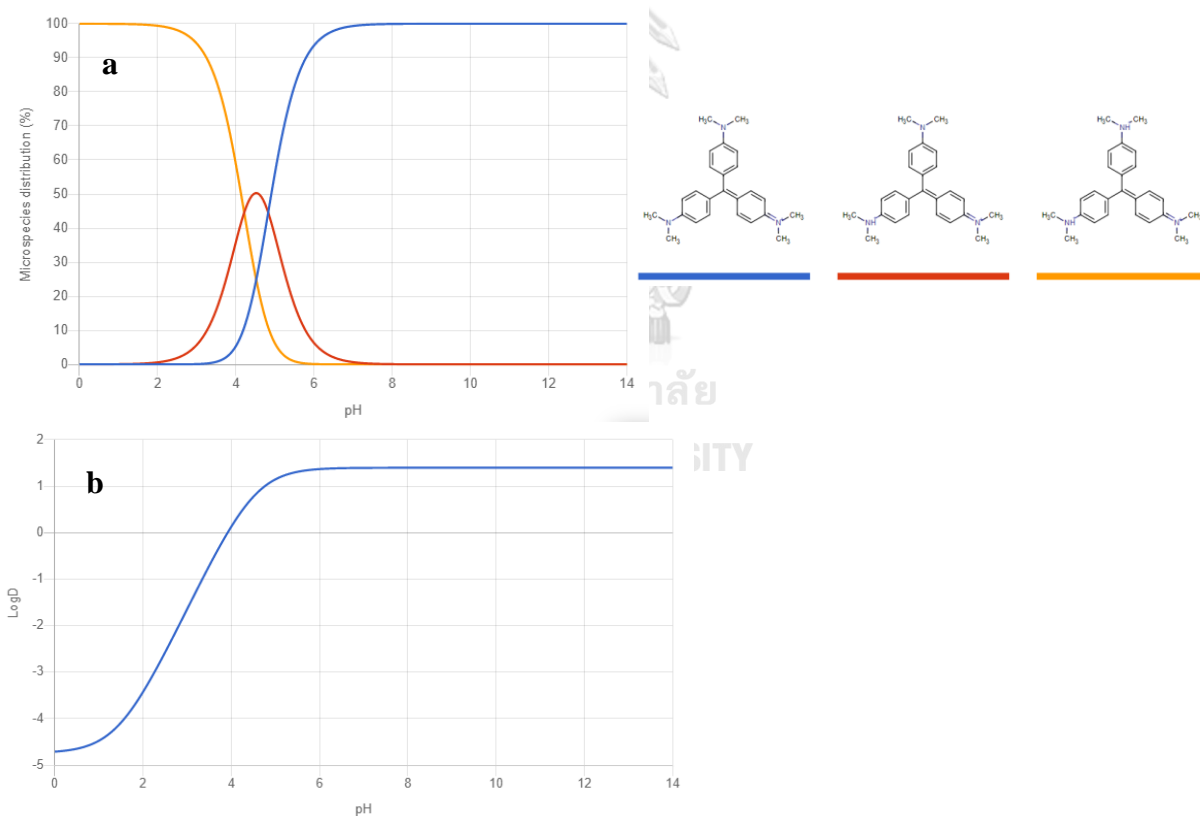


Figure 26. Crystal violet (a) microspecies distribution graph and (b) lipophilicity-pH graph (Chemicalize was used for calculating this property on 21 June 2022, <https://chemicalize.com/>, developed by ChemAxon)

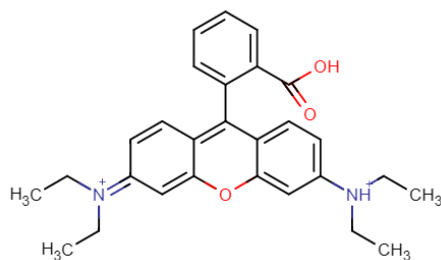


Figure 27. Dominant rhodamine B molecular structure in pH<3.5

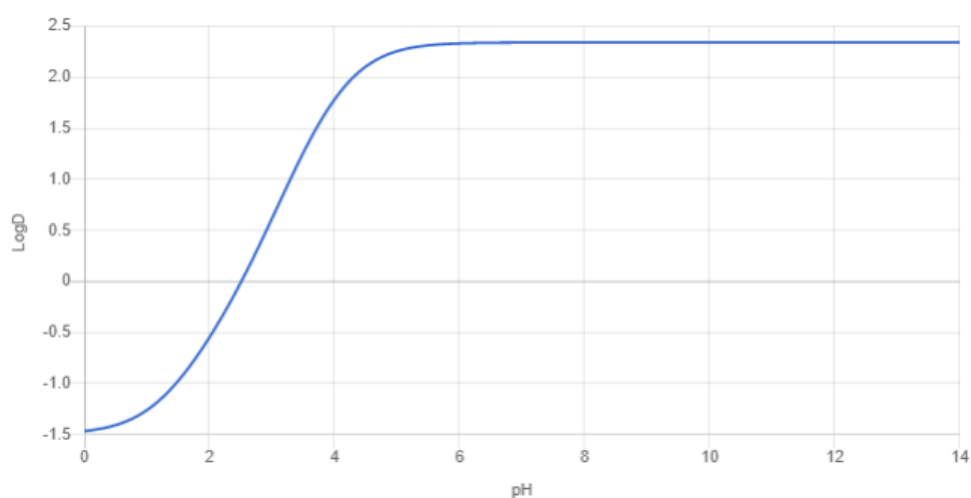


Figure 28. Diagram of pH-lipophilicity of rhodamine B (Chemicalize was used for calculating this property on 21 June 2022, <https://chemicalize.com/>, developed by ChemAxon)

Table 10. One-way ANOVA result of ROI area

Area (px ²)	RhB				CV			
	Mean intensity				Mean intensity			
	1	2	3	Average	1	2	3	average
100	197.33	196.23	197.34	196.97	183.92	184.36	186.22	184.83
200	196.30	195.99	197.22	196.50	184.69	185.36	185.64	185.23
400	195.89	196.72	196.34	196.32	185.53	185.76	186.10	185.80
1000	197.18	197.33	195.98	196.83	186.24	185.67	186.11	186.01
2000	196.96	196.99	197.00	196.98	185.60	186.89	185.69	186.06
mean	196.72				185.58			
SD	0.30				0.53			
%RSD	0.15				0.29			
P-value	0.94				0.32			

Table 11. List of dyes in the samples that is analyzed

Name of the dye	Class of dyes	of Exist in sample	Lipophilicity in pH 8
Allura red AC (INS 129)	Azo	Beverage and candy no. 6	LogD = -1
Ponceau 4R (INS 124)	Azo	Candy no. 4 and jelly	LogD = -3.5
Tartrazine	Azo	Candy no. 6	LogD = -8
Betanin	Alkaloid	Candy no. 1	LogD = -11
Anthocyanin peonidin-3-O-galactoside	Anthocyanin	Candy no. 5	LogD = -2

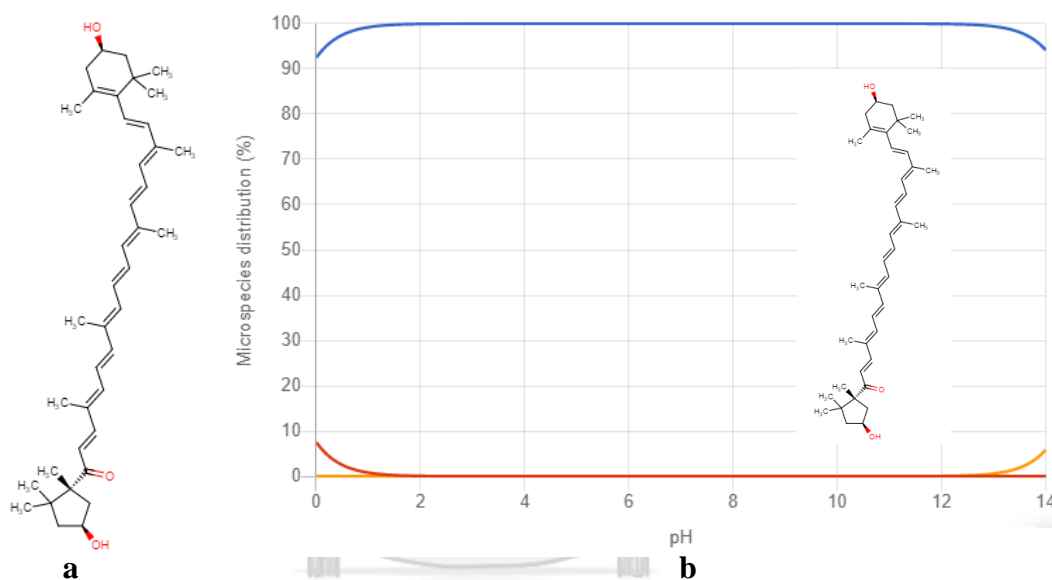


Figure 29. Figure of (a) molecular structure of capsanthin (b) the microspecies distribution of capsanthin in various pH (Chemicalize was used for calculating this property on 11 September 2022, <https://chemicalize.com/>, developed by ChemAxon)

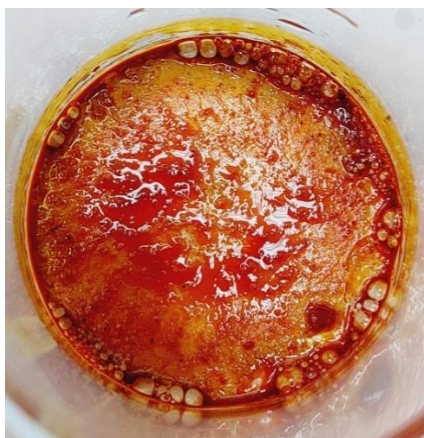


Figure 30. Residue from the extract from chili powder sample



Figure 31. figures of (a) aqueous extract from chili (b) microextraction result of aqueous extract



Figure 32. River water sample



Figure 33. Spike river water before filtration with 0 (non-spiked); 1 (10 $\mu\text{g/L}$); 2 (20 $\mu\text{g/L}$)

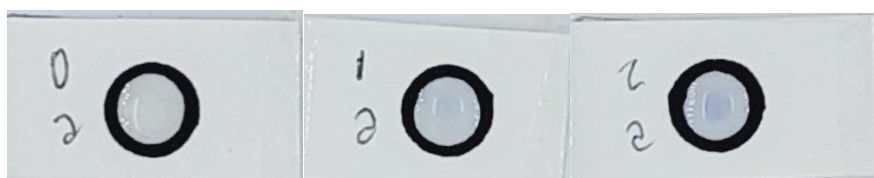


Figure 34. Spike river water after filtration with 0 (non-spiked); 1 (10 $\mu\text{g/L}$); 2 (20 $\mu\text{g/L}$)

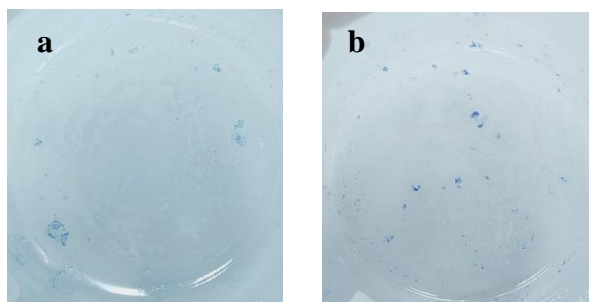


Figure 35. The precipitation on the spiked sample (a) 1 $\mu\text{g/g}$ and (b) 2 $\mu\text{g/g}$



REFERENCES

- (1) Ntrallou, K.; Gika, H.; Tsochatzis, E. Analytical and sample preparation techniques for the determination of food colorants in food matrices. *Foods* **2020**, *9* (1), 58.
- (2) Cheruiyot, G. K.; Wanyonyi, W. C.; Kiplimo, J. J.; Maina, E. N. Adsorption of toxic crystal violet dye using coffee husks: equilibrium, kinetics and thermodynamics study. *Scientific African* **2019**, *5*, e00116.
- (3) Li, Y.; Li, X.; Tang, S.; Yang, Y. Emulsification liquid–liquid micro-extraction based on natural deep eutectic solvent for (triarylmethane) dyes determination. *Chemical Papers* **2020**, *74* (10), 3617-3626.
- (4) ÖZKANTAR, N.; Soylak, M.; Tüzen, M. Spectrophotometric detection of rhodamine B in tap water, lipstick, rouge, and nail polish samples after supramolecular solvent microextraction. *Turkish Journal of Chemistry* **2017**, *41* (6), 987-994.
- (5) Prado, M.; Godoy, H. Validation of the methodology to determine synthetic dyes in foods and beverages by HPLC. *Journal of liquid chromatography & related technologies* **2002**, *25* (16), 2455-2472.
- (6) Shi, J.; Chen, L. Determination of rhodamine B in lipsticks by high performance liquid chromatography after extraction with AOT reversed micelles. *Analytical Methods* **2014**, *6* (21), 8627-8632.
- (7) Yang, Y.; Zhang, J.; Shao, B. Quantitative analysis of fourteen synthetic dyes in jelly and gummy candy by ultra performance liquid chromatography. *Analytical Methods* **2014**, *6* (15), 5872-5878.
- (8) Prado, M. A.; Boas, L. F. V.; Bronze, M. R.; Godoy, H. T. Validation of methodology for simultaneous determination of synthetic dyes in alcoholic beverages by capillary electrophoresis. *Journal of Chromatography A* **2006**, *1136* (2), 231-236.
- (9) Li, W.; Zhang, R.; Wang, H.; Jiang, W.; Wang, L.; Li, H.; Wu, T.; Du, Y. Digital image colorimetry coupled with a multichannel membrane filtration-enrichment technique to detect low concentration dyes. *Analytical methods* **2016**, *8* (14), 2887-2894.
- (10) Moradi, M.; Yamini, Y.; Ebrahimpour, B. Emulsion-based liquid-phase microextraction: a review. *Journal of the Iranian Chemical Society* **2014**, *11* (4), 1087-1101.
- (11) Moradi, M.; Yamini, Y. Surfactant roles in modern sample preparation techniques: a review. *Journal of Separation Science* **2012**, *35* (18), 2319-2340.
- (12) Mansour, F. R.; Khairy, M. A. Pharmaceutical and biomedical applications of dispersive liquid–liquid microextraction. *Journal of Chromatography B* **2017**, *1061*, 382-391.
- (13) Yamini, Y.; Rezazadeh, M.; Seidi, S. Liquid-phase microextraction–The different principles and configurations. *TrAC Trends in Analytical Chemistry* **2019**, *112*, 264-272.
- (14) Fameau, A.-L.; Arnould, A.; Saint-Jalmes, A. Responsive self-assemblies based on fatty acids. *Current opinion in colloid & interface science* **2014**, *19* (5), 471-479.
- (15) Sun, X.; Zhang, Z. Optimizing the novel formulation of liposome-polycation-DNA complexes (LPD) by central composite design. *Archives of pharmacal research* **2004**, *27* (7), 797-805.

- (16) Ramos, L. Critical overview of selected contemporary sample preparation techniques. *Journal of Chromatography A* **2012**, *1221*, 84-98.
- (17) Anastas, P.; Eghbali, N. Green chemistry: principles and practice. *Chemical Society Reviews* **2010**, *39* (1), 301-312.
- (18) Lord, H.; Pawliszyn, J. Evolution of solid-phase microextraction technology. *Journal of Chromatography A* **2000**, *885* (1-2), 153-193.
- (19) Rezaee, M.; Yamini, Y.; Faraji, M. Evolution of dispersive liquid-liquid microextraction method. *Journal of Chromatography A* **2010**, *1217* (16), 2342-2357.
- (20) Farajzadeh, M. A.; Mogaddam, M. R. A.; Aghdam, A. A. Comparison of air-agitated liquid-liquid microextraction technique and conventional dispersive liquid-liquid micro-extraction for determination of triazole pesticides in aqueous samples by gas chromatography with flame ionization detection. *Journal of Chromatography A* **2013**, *1300*, 70-78.
- (21) Salager, J.-L. Surfactants types and uses. *FIRP booklet* **2002**, 300.
- (22) Arnould, A.; Cousin, F.; Salonen, A.; Saint-Jalmes, A.; Perez, A.; Fameau, A.-L. Controlling foam stability with the ratio of myristic acid to choline hydroxide. *Langmuir* **2018**, *34* (37), 11076-11085.
- (23) Fan, Y.; Li, J.; Guo, Y.; Xie, L.; Zhang, G. Digital image colorimetry on smartphone for chemical analysis: A review. *Measurement* **2021**, *171*, 108829.
- (24) Jing, X.; Wang, H.; Huang, X.; Chen, Z.; Zhu, J.; Wang, X. Digital image colorimetry detection of carbaryl in food samples based on liquid phase microextraction coupled with a microfluidic thread-based analytical device. *Food chemistry* **2021**, *337*, 127971.
- (25) Peng, B.; Chen, G.; Li, K.; Zhou, M.; Zhang, J.; Zhao, S. Dispersive liquid-liquid microextraction coupled with digital image colorimetric analysis for detection of total iron in water and food samples. *Food chemistry* **2017**, *230*, 667-672.
- (26) Choodum, A.; Sriprom, W.; Wongniramaikul, W. Portable and selective colorimetric film and digital image colorimetry for detection of iron. *Spectrochimica Acta Part A: Molecular and Biomolecular Spectroscopy* **2019**, *208*, 40-47.
- (27) Ardila-Leal, L. D.; Poutou-Piñales, R. A.; Pedroza-Rodríguez, A. M.; Quevedo-Hidalgo, B. E. A brief history of colour, the environmental impact of synthetic dyes and removal by using laccases. *Molecules* **2021**, *26* (13), 3813.
- (28) Sahraei, R.; Farmany, A.; Mortazavi, S. A nanosilver-based spectrophotometry method for sensitive determination of tartrazine in food samples. *Food chemistry* **2013**, *138* (2-3), 1239-1242.
- (29) Ali, H. Biodegradation of synthetic dyes—a review. *Water, Air, & Soil Pollution* **2010**, *213* (1), 251-273.
- (30) Eisapour, M.; Shemirani, F.; Majidi, B. The ultratrace detection of crystal violet in fish and environmental water samples using cold-induced aggregation microextraction based on ionic liquid (IL-CIAME). *Analytical Methods* **2013**, *5* (20), 5731-5736.
- (31) Hayat, M.; Shah, A.; Hakeem, M. K.; Irfan, M.; Haleem, A.; Khan, S. B.; Shah, I. A designed miniature sensor for the trace level detection and degradation studies of the toxic dye Rhodamine B. *RSC advances* **2022**, *12* (25), 15658-15669.
- (32) Baldev, E.; MubarakAli, D.; Ilavarasi, A.; Pandiaraj, D.; Ishack, K. A. S. S.;

- Thajuddin, N. Degradation of synthetic dye, Rhodamine B to environmentally non-toxic products using microalgae. *Colloid Surface B* **2013**, *105*, 207-214. DOI: 10.1016/j.colsurfb.2013.01.008.
- (33) Authority, E. F. S. Opinion of the Scientific Panel on food additives, flavourings, processing aids and materials in contact with food (AFC) to review the toxicology of a number of dyes illegally present in food in the EU. *EFSA Journal* **2005**, *3* (9), 263.
- (34) Lin, S.; Lin, X.; Lou, X.-T.; Yang, F.; Lin, D.-Y.; Lu, Z.-W. Rapid and sensitive SERS method for determination of Rhodamine B in chili powder with paper-based substrates. *Analytical methods* **2015**, *7* (12), 5289-5294.
- (35) Kumari, M.; Gupta, S. K. Response surface methodological (RSM) approach for optimizing the removal of trihalomethanes (THMs) and its precursor's by surfactant modified magnetic nanoadsorbents (sMNP)-An endeavor to diminish probable cancer risk. *Scientific Reports* **2019**, *9* (1), 1-11.
- (36) Bhattacharya, S. Central composite design for response surface methodology and its application in pharmacy. In *Response surface methodology in engineering science*, IntechOpen, 2021.
- (37) Octanoic acid - Product type 18 (Insecticides, acaricides and products to control other arthropods). 2013; p 69.
- (38) Decanoic acid - Product type 4 (Food and feed area disinfectants). 2013; p 74.
- (39) Caleb, J.; Alshana, U. Supramolecular solvent-liquid-liquid microextraction followed by smartphone digital image colorimetry for the determination of curcumin in food samples. *Sustainable Chemistry and Pharmacy* **2021**, *21*, 100424.
- (40) Tan, J.; Li, M.-F.; Li, R.; Jiang, Z.-T.; Tang, S.-H.; Wang, Y. Front-face synchronous fluorescence spectroscopy for rapid and non-destructive determination of free capsanthin, the predominant carotenoid in chili (*Capsicum annuum* L.) powders based on aggregation-induced emission. *Spectrochimica Acta Part A: Molecular and Biomolecular Spectroscopy* **2021**, *255*, 119696.
- (41) Rai, M.; Hussain, S.; Pathan, M. A. A.; Farooqui, M. Adsorption Studies of Crystal Violet on Sand. *Asian Journal of Research in Chemistry* **2011**, *4* (6), 890-892.
- (42) Santhanalakshmi, J.; Balaji, S. Binding studies of crystal violet on proteins. *Colloids and Surfaces A: Physicochemical and Engineering Aspects* **2001**, *186* (3), 173-177.
- (43) Li, H.; Yin, J.; Liu, Y.; Shang, J. Effect of protein on the detection of fluoroquinolone residues in fish meat. *Journal of agricultural and food chemistry* **2012**, *60* (7), 1722-1727.
- (44) Acosta, G.; Talio, M. C.; Luconi, M. O.; Hinze, W. L.; Fernández, L. P. Fluorescence method using on-line sodium cholate coacervate surfactant mediated extraction for the flow injections analysis of Rhodamine B. *Talanta* **2014**, *129*, 516-522.
- (45) Zhou, Z.; Fu, Y.; Qin, Q.; Lu, X.; Shi, X.; Zhao, C.; Xu, G. Synthesis of magnetic mesoporous metal-organic framework-5 for the effective enrichment of malachite green and crystal violet in fish samples. *Journal of Chromatography A* **2018**, *1560*, 19-25.

VITA

NAME	Niluh Indria Wardani
DATE OF BIRTH	27 May 1997
PLACE OF BIRTH	Ujung Pandang
INSTITUTIONS ATTENDED	Hasanuddin University
HOME ADDRESS	Cozy Bangkok Place, 41/146-148, Soi. SUnthhhonpimol, Rama 4 Road, Rongmuang, Phatumwan, Bangkok, Thailand 10330
PUBLICATION	Wardani, N I, Ali S, Waleed A, Pakorn V, Solidified-surfactant-based microextraction coupled with digital colorimetric analysis on a paper platform for determination of rhodamine B in chili powder, Pure and Applied Chemistry International Conference: Proceeding (PACCON 2022). Alahmad, W, Nuttapat P, Thirawan B, Fatima A, Niluh I W, Pakorn V, Purge a trap in-tube colorimetric detection method for the determination of ethanol in alcoholic and non-alcoholic beverages, Advances in Sample Preparation, 4, 2022.
AWARD RECEIVED	Rector's Award for Best Graduate of Mathematics and Natural Sciences Faculty Hasanuddin University Period I 2019/2020 Dean's Award for Best Graduate of Chemistry Department Hasanuddin University Period I 2019/2020